Development of Superior Sorbents for Separation of CO_2 from Flue Gas at a Wide Temperature range during Coal Combustion

Final Technical Report

Reporting Period Start Date: July 1, 2003
Reporting Period End Date: June 30, 2007

by

Panagiotis G. Smirniotis

DoE Award Number: DE-FG26-03NT41810

Chemical & Materials Engineering Department
497 Rhodes Hall
University of Cincinnati
Cincinnati, OH 45221-0012

DISCLAIMER

No patentable subject matter is disclosed in this report.

Acknowledgements

The authors acknowledge U.S. Department of Energy for financial support (Grant Number # DE-FG26-03-NT41810) and Dr. Jose Figueroa of US DOE (NETL) for very fruitful discussions. We also thank Dr. S. Pratsinis and Mr. F. Ernest in ETH, Switzerland for help in synthesis of aerosol sorbents.

Abstract

In **chapter 1**, the studies focused on the development of novel sorbents for reducing the carbon dioxide emissions at high temperatures. Our studies focused on cesium doped CaO sorbents with respect to other major flue gas compounds in a wide temperature range. The thermo-gravimetric analysis of sorbents with loadings of CaO doped on 20 wt% cesium demonstrated high CO_2 sorption uptakes (up to 66 wt% CO_2/sorbent). It is remarkable to note that zero adsorption affinity for N_2, O_2, H_2O and NO at temperatures as high as 600 °C was observed. For water vapor and nitrogen oxide we observed a positive effect for CO_2 adsorption. In the presence of steam, the CO_2 adsorption increased to the highest adsorption capacity of 77 wt% CO_2/sorbent. In the presence of nitrogen oxide, the final CO_2 uptake remained same, but the rate of adsorption was higher at the initial stages (10%) than the case where no nitrogen oxide was fed.

In **chapter 2,** $Ca(NO_3)_2 \cdot 4H_2O$, CaO, $Ca(OH)_2$, $CaCO_3$, and $Ca(CH_3COO)_2 \cdot H_2O$ were used as precursors for synthesis of CaO sorbents on this work. The sorbents prepared from calcium acetate ($CaAc_2$-CaO) resulted in the best uptake characteristics for CO_2. It possessed higher BET surface area and higher pore volume than the other sorbents. According to SEM images, this sorbent shows "fluffy" structure, which probably contributes to its high surface area and pore volume. When temperatures were between 550 and 800 ^oC, this sorbent could be carbonated almost completely. Moreover, the carbonation progressed dominantly at the initial short period. Under numerous adsorption-desorption cycles, the $CaAc_2$-CaO demonstrated the best reversibility, even under the existence of 10 vol % water vapor. In a 27 cyclic running, the sorbent sustained fairly high carbonation conversion of 62%. Pore size distributions indicate that their pore volume decreased when experimental cycles went on. Silica was doped on the $CaAc_2$-CaO in various weight percentages, but the resultant sorbent did not exhibit better performance under cyclic operation than those without dopant.

Calcium oxides synthesized by flame spray pyrolysis and high temperature calcination were compared as sorbents of carbon dioxide. Flame made sorbents are solid nanoparticles with specific surface areas as high as 68 m^2/g. At 700 ^oC, all sorbents showed comparable fast carbonation rates during the first minutes and comparable maximum conversion with carbon dioxide during five hours adsorption. All samples showed high carbonation conversion of more than 95% over the first

In **chapter 3,** the Calcium-based carbon dioxide sorbents were made in the gas phase by flame spray pyrolysis (FSP) and compared to the ones made by standard high temperature calcination (HTC) of selected calcium precursors. The FSP-made sorbents were solid nanostructured particles having twice as large specific surface area (40-60 m^2/g) as the HTC-made sorbents (i.e. from calcium acetate monohydrate). All FSP-made sorbents showed high capacity for CO_2 uptake at high temperatures (773-1073 K) while the HTC-made ones from calcium acetate monohydrate

($CaAc_2 \cdot H_2O$) demonstrated the best performance for CO_2 uptake among all HTC-made sorbents. At carbonation temperatures less than 773 K, FSP-made sorbents demonstrated better performance for CO_2 uptake than all HTC-made sorbents. Above that, both FSP-made, and HTC-made sorbents from $CaAc_2 \cdot H_2O$ exhibited comparable carbonation rates and maximum conversion. In multiple carbonation/decarbonation cycles, FSP-made sorbents demonstrated stable, reversible and high CO_2 uptake capacity sustaining maximum molar conversion at about 50% even after 60 such cycles indicating their potential for CO_2 uptake.

Calcium-based sorbents with dopants of silica, titania, and zirconia with various ratios of dopant to calcium were also synthesized by FSP and discussed in **chapter 4**. The sorbents doping with zirconia gave the best performance among sorbents having different dopants. All Si/Ca, Ti/Ca, and most Zr/Ca sorbents showed performance deterioration during long term running except for the Zr/Ca (3/10). The one having Zr to Ca of 3:10 by molar gave stable performance. The calcium conversion kept stable around 64% during 102-cycle operations at 973 K. When carbonation was performance at 823 K, the Zr/Ca sorbent (3:10) exhibited stable performance of 56% by calcium molar conversion, or 27% by sorbent weight, both of which are less than those at 973 K as expected.

In **chapter 4** we investigated the performance of CaO sorbents with dopant by flame spray pyrolysis at higher temperature. The results show that the sorbent with zirconia gave best performance among sorbents having different dopants. The one having Zr to Ca of 3:10 by molar gave stable performance. The calcium conversion around 64% convession during 102-cycle operations at 973 K. When carbonation was performance at 823 K, the Zr/Ca sorbent (3:10) exhibited stable performance of 56% by calcium molar conversion, or 27% by sorbent weight, both of which are less than those at 973 K as expected.

In **chapter 5** we investigated the performance of CaO sorbents by flame spray pyrolysis at higher temperature with much shorter duration period. Stable high conversions were attained after 40 cycles The results show that the sorbent could reach high CO_2 capture capacity, be completely regenerated in short time and be quite stable even at these severe conditions.

Several studies were devoted to identify sorbents which could effectively capture CO_2 while survive in SO_2 atmosphere. From the group of sorbents we checked, a couple of sorbents showed very promising behavior, namely CO_2 uptakes higher than 60 % (wt/wt sorbent) while they acquired higher than 95% of their original activity/performance characteristics in a short period of time.

Contents

List of Acronyms and Abbreviations

FSP:	flame spray pyrolysis
HTC:	high temperature calcination
KJS:	Kruk-Jaroniec-Sayari
SEM :	Scanning electron microscopy
SCR:	Selective Catalytic Reduction
TGA:	Thermo Gravimetric Analyzer
TAGS:	Thermal Analysis Gas Station
TPO:	Temperature Programmed Oxidation
TPD:	Temperature Programmed Desorption
TCD:	Thermal Conductivity Detector
WGS:	Water Gas Shift reaction
XPS:	X-ray Photoelectron Spectroscopy

Tables and Figures

desorption, 700 ^{o}C; Concentration of gases, a, 30 vol % CO_2 balanced by helium; b, 10 vol % H_2O (gas) + 30 vol % CO_2 balanced by helium.
Figure 2.10. Pore size distribution of $CaAc_2$-CaO sorbents: after adsorption and desorption at 700 ^{o}C.
Figure 2.11. Maximum adsorption values of CO_2 over $CaAc_2$-CaO sorbents doped with 0 to 50 wt % SiO_2. Conditions: Temperature of adsorption-desorption, 700 ^{o}C; Concentration of CO_2, 30 vol % balanced by helium
Figure 3.1. XRD patterns of as prepared FSP-made sorbents (Table 1). The sharp spectra and rather flat baseline indicate that these are crystalline materials.
Figure 3.2. Thermogravimetric analysis of the pretreatment of FSP-made sorbents (Table 1) showing the release of adsorbed H_2O (~600 K) and $CaCO_3$ (~800 K) conversion.
Figure 3.3. Carbonation/decarbonation cycles on FSP-made sorbents (Table 1) at 973 K showing high capacity and reversible reactions. Carbonation/decarbonation Time: 300 min/30 min.
Figure 3.4. The evolution of the maximum carbonation conversion of FSP-made sorbents (Table 1) with the number of carbonation/decarbonation cycles (60 min /30 min) at 973 K. Stable high conversions were attained after 40 cycles.
Figure 3.5. TEM Images of (a) FSP3-CaO, (b) HTC $CaCO_3$-CaO, (c) FSP3-CaO after one cycle at 973 K, and (d) HTC $CaCO_3$-CaO after one cycle at 973 K. Images indicate that FSP-CaO sorbents are nanoparticles, and both FSP-, and $CaCO_3$-CaO sorbents sintered after reactions.
Figure 3.6. Conversion of three HTC-made sorbents at 773 K and 973 K, respectively, indicating the high SSA and porous structure of the $CaAc_2$-CaO sorbents related to their high performance.
Figure 3.7. Pore size distribution of HTC-made sorbents from various precursors.
Figure 3.8. Thermogravimetric analysis of $CaAc_2 \cdot H_2O$ sorbent calcination indicating that its characteristic structure arose from specific multi-step decompositions.
Figure 3.9. Conversion of FSP3-CaO and $CaCO_3$-CaO at 973 K indicating that the high SSA of the former induced the fast reaction and high conversion.
Figure 3.10. Uptake of CO_2 by FSP3-CaO and $CaAc_2$-CaO at various temperatures.
Figure 3.11. Carbonation/decarbonation (300 min/30 min) cycles on FSP3-CaO and $CaAc_2$-CaO at 973 K showing that the former sustained carbonation around 50% after the 20^{th} cycle
Figure 4.1. Carbonation/decarbonation (30 min/30 min) cycles on Si/Ca(1/10), Ti/Ca(1/10), and Zr/Ca(1/10) sorbents at 973 K showing that the Zr doped sorbents have better performance both in conversion and durability.
Figure 4.2. Carbonation/decarbonation (30 min/30 min) cycles on flame-made Zr/Ca sorbents having various Zr/Ca ratios at 973 K showing that a sorbent's performance could be stable even after 102-cycle running when it has a Zr/Ca ratio of 3/10.
Figure 4.A1. 102 Operation cycles with Zr/Ca made by flame: original TGA figure. Sorbent: Zr/Ca=3:10 (atomic ratio); carbonation /decarbonation temperatures: 973 K (700 ^{o}C); carbonation/decarbonation time: 30 min/30 min.
Figure 4.A2. 52 Operation cycles with Zr/Ca made by flame: original TGA figure. Sorbent: Zr/Ca=3:10 (atomic ratio); carbonation /decarbonation temperatures: 550 ^{o}C/700 ^{o}C (823 K/973 K); carbonation/decarbonation time: 30 min/30 min.
Figure 5.1. Carbonation/decarbonation (5 min/5 min) cycles on FSP1-CaO at a. 973 K, b. 1073 K and c. carbonation for 5 min at 973 and decarbonation for 40 minutes from 973 K to 1173 K and from 1173 K back to 973 K both at 10 K/min. The sorbent

could reach high CO_2 capture capacity, be completely regenerated in short time and be quite stable even at higher temperatures.

Figure 5.2. Intial carbonation performance of FSP-made CaO sorbent. There was 2 min delay time for CO_2 to reach reactor.

Figure 5.3. M_xO_y/CaO (1/10 by molar) performance at 30 % vol CO_2 Carbonation: 30 % vol CO_2; 1023 K; 60 min. Decarbonation: helium; 1023 K; 30 min.

Figure 5.4. M_xO_y/CaO (1/10 by molar) performance at 30 % vol CO_2 and 1000 ppmv SO_2. Carbonation: 30 % vol CO_2, 1000 ppmv SO_2, in helium; 1023 K; 60 min Decarbonation: helium; 1023 K; 30 min.

Chapter 1. Alkali Metals/CaO as Sorbents for CO_2: Parametric Study of Cs/CaO Sorbents at High Temperatures

Executive Summary

Cs/CaO based sorbents were synthesized, characterized with modern techniques and tested for sorption of CO_2 and selected gas mixtures simulating flue gas from coal fired boilers. Our studies resulted in highly promising sorbents since they demonstrated zero affinity for N_2, O_2, and NO, very low affinity for water (CO_2/H_2O ratios >100), high CO_2 sorption capacities at high temperatures, rapid sorption characteristics, CO_2 sorption at a very wide temperature range (50 to 650 ^oC), durability, and low synthesis cost. One of the "key" characteristics of the proposed materials is the fact that we can control very accurately their basicity (optimum number of basic sites of the appropriate strength) which allows for the selective chemisorption of CO_2 at a wide range of temperatures (50 to 650 ^oC). The unique characteristics of this family of sorbents offer high promise for development of advanced industrial sorbents for the effective CO_2 removal as well as other types of applications such as fuel cells, inorganic membranes, water gas shift reaction (WGS), and syngas applications.

The performed work constitutes about 20% of the proposed work and offers a screening for effectiveness in conjunction with the most important operating parameters. Our efforts fall within the budget.

Since we observed that our CaO sorbents behave satisfactorily with the most important gases of flue gas, our immediate efforts will concentrate on studying numerous types of composite sorbents based on CaO (SiC was considered, various sol-gel made, ceramic foams, and aerosol made materials) in order to come up with sorbents with superior durability. As part of our studies we will study the performance of CaO-based sorbents for CO_2 sorption cycles, regeneration efficiency.

Our long term plans for this project will be to test the best and most durable sorbents in the presence of SO_2. Moreover, we will test our sorbents at conditions used for WGS and syngas applications, gasification.

1.1. Introduction

The carbonation of CaO sorbents has been recently studied for the separation of carbon dioxide at high temperatures using industrial or natural limestone [1, 2, 3, 4]. The present paper continues our earlier work [4], in which we investigated CaO sorbents supported with alkali metals. It was found that for that family of sorbents which involved low BET surface area supports, the CO_2 sorption increases in the following order Li<Na<K<Rb<Cs. The optimum adsorption temperature for CO_2 in that work was 600°C since this temperature offered the highest sorption rate and high sorption uptake. The reason for the enhanced CO_2 adsorption affinity observed was the increase of the basic nature of CaO sorbent with the addition of the alkali metal, particularly with cesium. Moreover, it was found [4], that CaO support doped with 20wt% cesium synthesized by CsOH precursors reached the highest CO_2 adsorption with respect the other precursors used.

The carbonation reaction on calcinated limestone is well investigated, but most of the studies have been performed under non-practical conditions such as absent of poisons or low temperature. Species such as H_2O, NO and particularly SO_2, can influence the CO_2 sorption on CaO-based sorbents. Borgwardt [5] investigated the influence of water on CaO sorbent and he reported that of increasing sorbent sintering effects. Although several studies have been carried out to investigate the effect of flue gas on pure CaO, to the best of our knowledge no investigation was performed for the direct influence of flue gas for CO_2 adsorption on alkali metal doped CaO sorbents.

We will study in this project the sorption performance of Cs/CaO sorbent for the major components of exhaust gases from coal fired power plants such as CO_2, N_2, O_2, NO, SO_2 and H_2O. We investigated the effects of both the individual compounds and selected gas mixtures simulating flue gas at various conditions (Table 1.1) as a preliminary effort to screen for effectiveness this family of sorbents. At this point it is essential that we note that this family of sorbents demonstrates significant sorption uptakes and very rapid kinetic characteristics at temperatures above about 400 ^oC (reaching as high as 700 ^oC). This characteristic is unique and offers the potential for these sorbents to be used at significantly higher temperatures for capture of CO_2 in the energy industries in general beyond the traditional way (removal of CO_2 after the FGD). With these sorbents, one can capture CO_2 before the air heater or the particle collector (Figure 1.1). Due to the ability of our sorbents to operate at high temperatures, we can use them right after the boiler to capture CO_2 from the hot stream of flue gas. A potential advantage of the latter proposal is that these sorbents might be able to capture Hg and other trace metals in addition to CO_2; something with obvious advantages for the remaining processes/reactors of the "purification train".
At this stage it should be noted that the increased effectiveness of these sorbents to capture selectively CO_2 at elevated temperatures (>550 ^oC) can be beneficial to other types of applications such as fuel cells, inorganic membranes, water gas shift reaction (WGS), and syngas applications.

1.2. Experimental

The test plan involves the evaluation of the Cs/CaO sorbent as a function of the key operating parameters. This study constitutes a screening for effectiveness of this sorbent and provides invaluable information for understanding the potential for the industrial realization of CO_2 capture.

1.2.1 Synthesis procedure

The alkali metal doped sorbents were prepared by the wet impregnation method using commercial CaO (Aldrich) support. The precursor used for the loading of cesium was CsOH (Aldrich, 50 wt% solution in water) since we found earlier [4] that this precursor leads in better sorbents. The sorbent was prepared by mixing the appropriate amount of alkali metal precursor and calcium oxide (in the order of grams) in order to reach cesium of 20wt% (based on cesium metal and CaO only). Distilled water was added for the formation of the slurry in the proportion of 1 gram of CaO to 100 g of aqueous solution of the alkali metal precursor. The slurry was heated and stirred until the water was evaporated. The powder was ground to fine powder and dried in an oven at 120 °C overnight. The calcination of sorbent was carried out under an oxygen atmosphere at 750 °C for 5 hours in order to reach a full oxidation of the cesium precursor. After the step of calcination, the sorbent were stored under inert atmosphere.

1.2.2 Particle size analysis

The particles-size distribution of the sorbent material was obtained (Figure 1.2) with a laser scattering particle distribution analyzer (Malvern Mastersizer S series). The instrument is accurate to within 5 % of the median value, as claimed by the manufacturer. Prior to the measurements, the sorbent was dispersed using ultrasound.

1.2.3. BET surface area and pore size measurements

BET surface area and pore size distribution measurements were performed using nitrogen adsorption and desorption isotherms at –196 °C on a Micromeritics ASAP 2010 volumetric adsorption analyzer. The sorbent samples were degassed at 300 °C for at least 5 hours in the degassing port of the apparatus. The pore size distribution was obtained from the branch of the isotherm using the KJS (Kruk-Jaroniec-Sayari) method [7]. An additional BET measurement was carried out in an AutoChem 2910 analyzer to determine the BET surface area before and after the water vapor injection by avoiding exposing the sorbents to the ambient atmosphere. The sorbent was pretreated at 750 °C for 5 hours in order to get a complete outgassed sorbent. In this manner, the sorbent is free of all pre-adsorbed atmospheric water or carbon dioxide. The results are presented in Table 1.3.

1.2.4. Sorption experiments

The adsorption and desorption experiments were carried out in a Perkin Elmer PYRIS-1 thermo gravimetric analyzer (TGA) equipped with thermal analysis gas station (TAGS). For the sorption experiments the samples were placed in a platinum sample holder. The sample-pan holder was batch operated with a single charge of about 5 mg.

Each experiment started with a pretreatment step, in order to degas the sorbent from pre-adsorb gases and water. The temperature profile of these experiments was consisted of a heating up step with a ramp of 10 °C/min to 750 °C, holding of the sample for 3 hours at 750 °C, and a cooling down step with a rate of 15 °C /min to the adsorption temperature. The pretreatment was carried under helium atmosphere. The adsorption experiments were carried out at the adsorption temperature of interest for 5 hours. The same characteristics were followed for a limited number of experiments we performed to investigate the cyclic operation of the sorbents. Prior to the adsorption experiments, the samples were held for 30 min at the adsorption temperature in helium flow in order to get a stable flow profile and baseline.

1.3. Results and discussion

Characteristic TGA curves of isothermal CO_2 adsorption over 20 wt% Cs/CaO sorbent are depicted in Figure 1.3 within a temperature range of 225 °C to 675 °C. A monotonic increase of CO_2 sorption was observed by increasing the temperatures. At relatively low temperatures the CO_2 chemisorption is low but the uptake increased significantly for temperatures above 450 °C. The maximum adsorption uptake was reached at 600 °C and was equal to 66 wt% CO_2/sorbent. Surprisingly, at 675 °C the CO_2 sorption is about 10 wt% lower in comparison with that at 600 °C. The reason is that the thermal stability of formed Cs_2CO_3 is limited for the bulk face to ~610°C [8]. Hence, when the adsorption and/or the desorption steps take place at temperature higher than 610 °C, the state of the sorbent significantly changes. Evidently, the ideal temperature for high temperature CO_2 adsorption using cesium-doped sorbents is around 600°C. XPS investigations performed by our group confirm the reactions of carbonation and desorption in the corresponding range, which are presented in equations (1-4).

Chemisorption

$$CaO + CO_2 \rightarrow CaCO_3 \quad (1)$$

$$Cs_2O + CO_2 \rightarrow Cs_2CO_3 \quad (2)$$

Desorption

$$CaCO_3 \rightarrow CaO + CO_2 \quad (3)$$

$$Cs_2CO_3 \rightarrow Cs_2O + CO_2 \quad (4)$$

The advantage of cesium doped CaO sorbent is clearly demonstrated in comparison to the CO_2 uptake on the pure CaO sorbent at 600 ^oC (dashed curves in Figure 1.3). This is due to the fact that cesium oxide leads to higher surface basicity, which favors the chemisorption of a weak acid such as CO_2.

A monotonic increase of the sorption uptakes is observed in the entire range of temperatures investigated. However, the uptake is very low at ambient temperature or temperatures slightly higher than ambient (Table 1.4). Our data demonstrate that the great potential of this family of sorbents occurs at elevated temperatures.

It is worth noting that the uptake of the sorbent reaches as high as 30 wt% CO_2/mass of sorbent within the first two minutes, a property of unique importance from kinetic point of view since it can result in rapid sorption/desorption cycles. This behavior is different, in comparison with our previous experimental observations [4] where a lower adsorption rate was observed. However, it can be justified by the use of different gas atmospheres during the calcinations. In our previous work [4] the sorbent was calcined under helium atmosphere and the CsOH precursor used was dehydrated but not fully oxidized. In the present set of experiments the calcinations were carried out under oxygen and resulted in the complete oxidation of the cesium precursor thus leading to the fully oxidized form of sorbent. Consequently, the surface characteristics of the present sorbents are completely different in comparison to those in our earlier work. Equations (5) and (6) present what is happening during the calcinations under the different atmospheres.

$$2CsOH \xrightarrow[Helium]{750\,^oC} Cs_2O + H_2O \quad (5)$$

$$4CsOH + 3O_2 \xrightarrow{750^{o}C} 4CsO_2 + 2H_2O \qquad (6)$$

During the wet impregnation method, only the excess water of the slurry was evaporated, the slurry becomes a solid material at ambient temperatures, and acquires the uniform dispersion of cesium on the sorbent. Hence, the uncalcined sorbents possess CsOH. Typical dehydration of CsOH (reaction 5) is only taking place during the calcinations at 750 °C under helium atmosphere. The CsOH is fully oxidized (reaction 6) and forms cesium superoxide, CsO_2 [9] layers on the sorbent surface, when calcined at 750 ^{o}C under oxygen atmosphere. Yagi and Hattori [10] investigated the oxygen adsorption on cesium-added zeolite X. They reported that Cs_2O adsorbs oxygen to form Cs_2O_3 and Cs_2O_4. TPO-TPD experiments of un-calcined sorbent under oxygen atmosphere were carried out in order to find out the temperature and phase of the cesium oxides formed in our sorbents. As shown in Figure 1.4 only one adsorption peak was found at 643 °C, which, corresponds, to CsO_2 as determined by total amount of oxygen consumed after integration of the TCD peaks. The CO_2 adsorption affinity of sorbents calcined under helium and oxygen (figure 1.5 and 1.6) was compared. It was observed that the sorbent calcined under oxygen atmosphere demonstrated significantly high adsorption compared to the sorbent calcined under helium. This difference was due to the formation of Cs_2O_3 phase in the sorbent during the calcination under oxygen atmosphere. Whereas, Cs_2O phase of cesium oxide was observed by XPS [4], when the sorbent was calcined under helium atmosphere. From these results it is well demonstrated that the sorbent calcined in oxygen with its full-oxidized cesium oxide (Cs_2O_3) enforce the rapid and significantly high amount of CO_2 adsorption.

Effect of N_2 and O_2

The results of the nitrogen and oxygen adsorption experiments were presented in Figure 1.3. It is remarkable to note that the sorbent shows zero affinity for both gases. This is the case for the entire range of temperatures we investigated varying from 50 to 600 ^{o}C. This demonstrates that the sorbent adsorbs only the gas molecules, which are of acidic nature. Neither of these two gases can react with the surface. More specifically, since the sorbent was calcined at 750 °C under O_2 atmosphere, it cannot further react with oxygen at 600 °C. On the other hand, our sorbents do not react with N_2 in a wide range of temperatures. This property is of unique importance for the development of highly selective CO_2 sorbents from a stream of flue gas utilizing any fossil fuels and air since the nitrogen and the unused O_2 will correspond to at least 70vol.% of the gases.

Effect of temperature on H_2O adsorption

The effect of temperature for water adsorption on our sorbents is presented in Figure 1.7. A rather "complicated" behavior is observed with respect to temperature due to the various reactions occurring. The reaction of water with calcium oxide, equation (7) is a well-known and keen process at ambient pressures and temperatures. In addition, the cesium oxide also possesses high adsorption affinity towards water since cesium oxide is the strongest known basic oxide, and it readily reacts with water to form CsOH, the reaction is shown in (8).

$$CaO + H_2O \rightarrow Ca(OH)_2 \qquad (7)$$
$$Cs_2O + H_2O \rightarrow 2CsOH \qquad (8)$$

Hence, at 225 °C $Ca(OH)_2$ [11] and CsOH layers were formed on the sorbent's surface due to high water adsorption, namely 27 wt% H_2O/mass of sorbent. However, with increasing sorption temperature a considerable decrease of the water adsorption was observed. This behavior continues monotonically up to the point where the sorbent exhibits a zero water adsorption affinity at temperatures equal or higher than 600 °C. The chemical explanation for the monotonic decrease of the adsorbed amount of water with increasing temperature is based on the continuously decreasing extent of reactions 6 and 7 with temperature. $Ca(OH)_2$ and CsOH completely decompose at temperatures higher than 580 °C [8]. Furthermore, the sorbents become more porous and acquire smaller particle sizes, which explains the significantly larger CO_2 adsorption capacity at high temperature in the presence of water. To some extent this phenomenon is somehow similar to the synthesis of activated carbons by water treatment. The influence of water for the surface chemistry on CaO was intensively investigated by Borgwardt [5] and supports our results, since it is reported that water vapor promotes the sorbent sintering and agglomeration. However, in the latter paper the authors only studied the first 10-20 min of the sintering process. Therefore, it was not clear if the final surface area was affected by water.

NO Influence

The results of the performance of adsorption experiments using nitrogen oxide are presented in Figure 1.8. A monotonic trend of decreasing NO adsorption affinity at rising temperatures was found. At relatively low temperatures (225 °C) a slight NO adsorption of 0.8 wt% NO/sorbent was obtained. The reason for this behavior is that nitrogen oxide is reacting with trace amounts of nondispersed cesium oxide on the sorbent surface. This compound is thermally stable up to 414 °C. At higher temperatures the decomposition of $CsNO_3$ takes place. The decomposition temperature of $CsNO_3$ is 450 °C, which means, the adsorption of NO is not possible beyond this temperature. This might be the reason for the negligible increase of the sorbent's weight at this temperature. However, in the presence of nitrogen oxide a loss in sorbent weight was observed at high temperatures and particularly at 675 °C due to the decomposition of $CsNO_3$ into metallic cesium. Because of this phenomenon a rapid adsorption of CO_2 was observed in the presence of NO (Figure 1.9).

The promising adsorption characteristics of the cesium doped calcium oxide with its high CO_2 adsorption capacity, zero adsorption affinity for water, nitrogen, oxygen and nitrogen oxide promise an advanced practical use for CO_2 separation from flue gas at high temperatures as 600 °C.

Effect of Various Gas Mixtures

Adsorption experiments with different mixtures of CO_2 and other compounds found in flue gas (H_2O, N_2, O_2) were tested to investigate the effect of the flue gas composition on the CO_2 adsorption at 600 °C. Our results presented in Figure 1.9 show that nitrogen and oxygen have no effect for the CO_2 adsorption since we observed the same adsorption capacity with the case of using only CO_2 (Figure 1.9), where 66 wt% CO_2/sorbent was reached under identical operating conditions. This finding offers a chance for highly selective CO_2 separation if one considers that nitrogen is the component flue gas with a highest concentration (<75vol%). In addition, it was observed that nitrogen oxide does not have any negative influence for the carbon dioxide adsorption. The results in Figure 1.9 furthermore demonstrate that the water vapors affected significantly, namely increase the CO_2 adsorption. In the presence of 10vol% water, the highest adsorption 77wt% CO_2/sorbent after 5 h

adsorption time was recorded. The fact that the sorbent particle size decreased after water adsorption (see Table 1.2) clearly indicates that the sorbent is more porous than prior to the water adsorption. It might be that the water vapor increases the porosity of the sorbent and acquire uniform pore diameter (see Figure 1.10). This enhances the high CO_2 adsorption, due to the fact that the building of Cs_2CO_3 $CaCO_3$ layers is not able to plug the pore mouths. In this manner, the diffusion of CO_2 is enhanced into the core levels of the sorbent. Gupta and Fan [1] also reported low surface area CaO sorbents, which, demonstrated high CO_2 uptake due to larger pore diameters. The pore diameter and pore size distribution of our sorbents treated in different environment are shown in Figure 1.10. The addition of NO and water at high temperatures promotes the formation of uniform pore size distribution, which causes the more effective sorbent towards CO_2 adsorption. In addition, Shimizu and Inagaki [12] reported that water affect higher mobility of Ca^{2+} and O^{2-} and this enhanced higher reaction with acidic gases as CO_2.

The result of the particle size distribution after the calcinations and after the addition of CO_2, H_2O and NO are depicted in Figure 1.2. The mean particle sizes are summarized in Table 1.2. As one can observe the mean particle size of the non-calcined sorbent is the largest after O_2 calcination. The increasing of sorbent particle size might be due to the formation cesium super oxide on the surface of the sorbent during the calcinations under oxygen atmosphere. The particle size decreased in the presence of NO and water during the calcination. It can be explained due to the formation of a mesoporous type of sorbent in the presence of NO and water. The largest particle size was found for the sample after CO_2 adsorption, reasonable by the formation of $CaCO_3$ and Cs_2CO_3 particle on the sorbent surface.

1.4. Conclusions

Experiments were preformed with 20wt% Cs/CaO sorbent in a TGA. The objective of these experiments was to verify the effect of CO_2 adsorption on the sorbent with consideration to flue gas conditions.

1) The carbonation rate of the new sorbent was improved reasonably by a full oxidation of the cesium support because of oxygen as calcination gas.
2) In order to develop selective adsorbents for carbon dioxide at high temperature our findings show a zero adsorption affinity for N_2, O_2, H_2O, NO at 600°C.
3) At high temperatures NO and H_2O promote sintering and shrinking effects by the fact that decreasing particle size and simultaneously forming uniform pore sizes
4) The presence of water vapor significantly promotes the CO_2 sorption capacity of the sorbent.
5) In the presence of nitrogen oxide a rapid CO_2 uptake was observed within the first two minutes.

1.5. Reference:

[1] H. Gupta, L. S. Fan
Carbonation-Calcination Cycle Using High Reactivity Calcium Oxide for Carbon Dioxide Separation from Flue Gas
Ind. Eng. Chem. Res. 2002, 41, 4035-4042

[2] C. Salvador, D. Lu, E.J. Anthony, J.C. Abanades
Enhancement of CaO for CO_2 capture in a FBC environment

Chemical Engineering Journal 96, 2003 187-195
[3] J. C. Abanades, D. Alvarez
Conversion Limits in the Reaction of CO_2 and Lime
Energy & Fuels 2003, 17, 308-315
[4] Ettireddy P. Reddy, Panagiotis G. Smirniotis
High Temperature Sorbents for CO_2 made of Alkali Metals doped CaO Supports
J. Physical Chemistry, 2004, 108, 7794-7800
[5] R. H. Borgwardt
Calcium Oxide Sintering in Atmospheres Containing Water and Carbon Dioxide
Ind. Eng. Chem. Res. 1989, 28, 493
[6] J. Armor
Environmental Catalysis
205th National ACS Meeting, p 206 (1994).
[7] M. Kurk, M. Jaroniec, A. Sayari
Application of Large pore MCM-41 Molecular sieves To Improve Pore Size Analysis Using Nitrogen Adsorption Measurements
Langmuir, 1997, Vol.13, 6267-6273
American Chemical Society
[8] D. R. Lide
CRC Hand Book of Physics and Chemistry, 84th Edition
CRC Press LLC, 2003-2004.
[9] A. R. West,
Basic solid state chemistry
John Wiley & Sons, 1999
[10] F. Yagi, H. Hattori
Oxygen Exchange Between Adsorbed Oxygen and Cesium-Added Zeolte X
Microporous Materials 1997, 9, 247-251
[11] K. Kuramoto, S. Fujimoto,
Repetitive Carbonation-Calcination of Ca-based Sorbents for Efficient CO_2 Sorption at Elevated Temperatures and Pressures
Ind. Eng. Chem. Res. 2003, 42, 975-981
[12] T. Shimizu, M. Inagaki.
Decomposition of N_2O over Limestone under Fluidized-Bed Combustion Conditions
Energy Fuels, 1993, 7, 648-654.

Table 1.1. Various gas mixtures used in this study

Type of Gas Mixture	Components	Composition, %
1	CO_2	28.6%
	H_2O	10.0%
	He	61.4%
2	CO_2	28.6%
	NO	0.4%
	He	71.0%
3	CO_2	28.6%
	SO_2	0.4%
	He	71.0%
4	CO_2	28.6%
	N_2	22.6%
	O_2	6.0%
	He	42.8%
5. Simulated flue gas	CO_2	11.0%
	H_2O	10.0%
	N_2	71.0%
	O_2	2.0%
	NO	0.05%
	SO_2	0.05%
	He	5.9%

Table 1.2. Mean particle sizes

Sorbent	Mean particle size μm
20wt%Cs/CaO (after O_2 calcination)	19.4
20wt%Cs/CaO (after H_2O adsorption)	11.2
20wt%Cs/CaO (after NO adsorption)	13.9
20wt%Cs/CaO (after CO_2 adsorption)	20.4

Table 1.3. BET surface area before and after H_2O injection on 20 wt% Cs/CaO

BET measurement	adsorbed volume Ml	sample amount mg	BET surface area m^2/g
1	0.431	101.1	18.57
2	0.313	101.1	13.49

Table 1.4. CO_2 captured at different temperature after 300 minutes of adsorption

Temperature	50°C	225°C	300°C	375°C	450°C	525°C
CO_2 captured/ gram sorbent	1.5grams	3.1grams	4.5grams	10.4grams	34.0grams	45.5grams

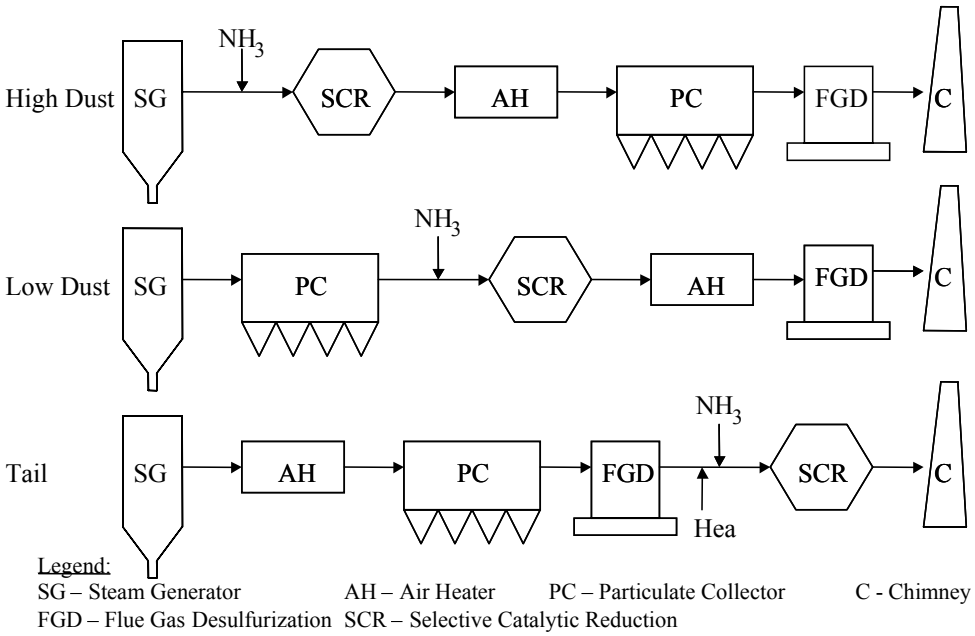

Figure 1.1. Various Configurations and Purification Procedures for Coal fired Plants (J. Armor, Environmental Catalysis, 205th National ACS Meeting, p. 206, 1994)

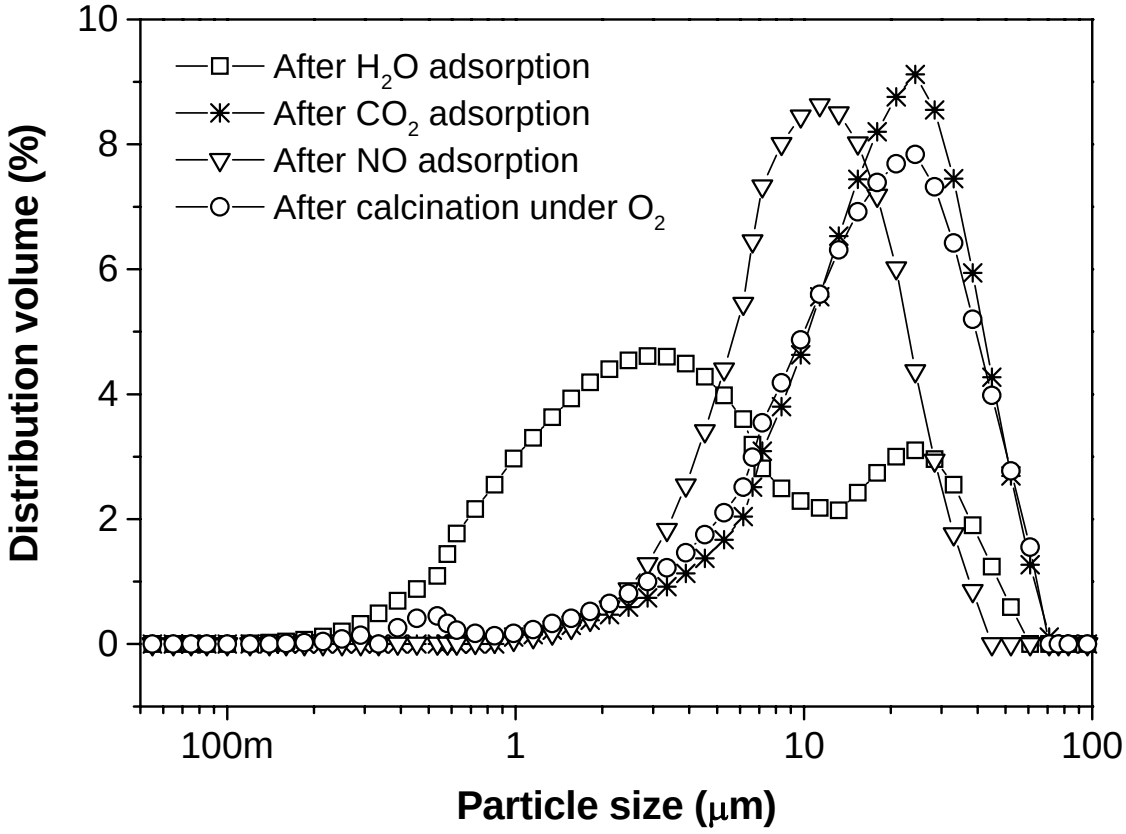

Figure 1.2. Particle size distribution of the sorbent 20wt.%Cs/CaO after calcinations at 750°C under and after adsorption of different gases at 600°C

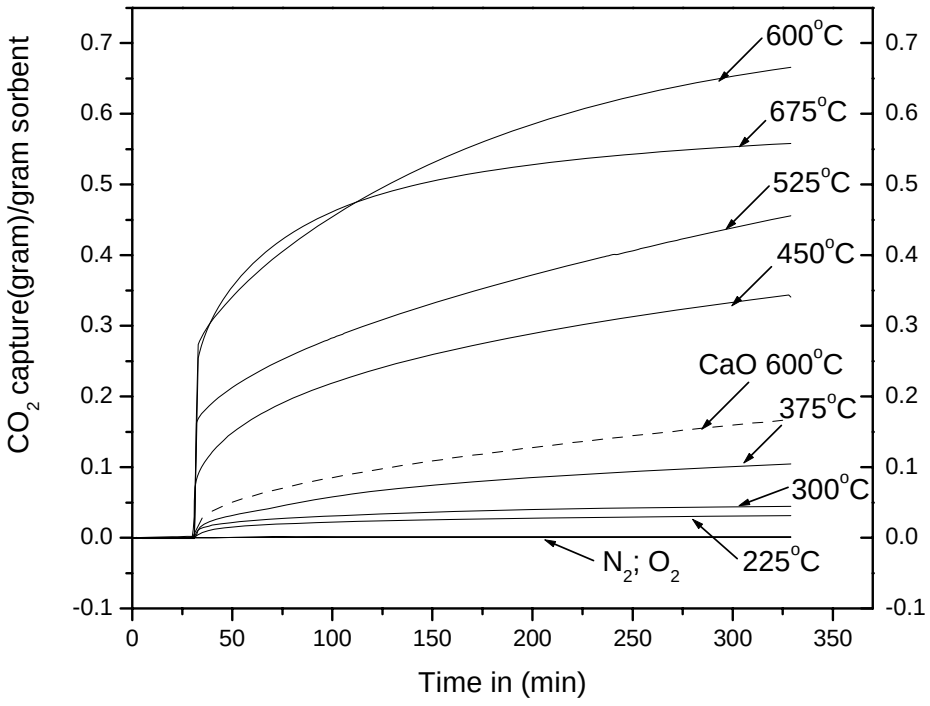

Figure 1.3. Effect of temperature for CO_2 adsorption over 20 wt% Cs/CaO: concentration of CO_2 = 28.6% balanced on helium; total flow = 70ml/min

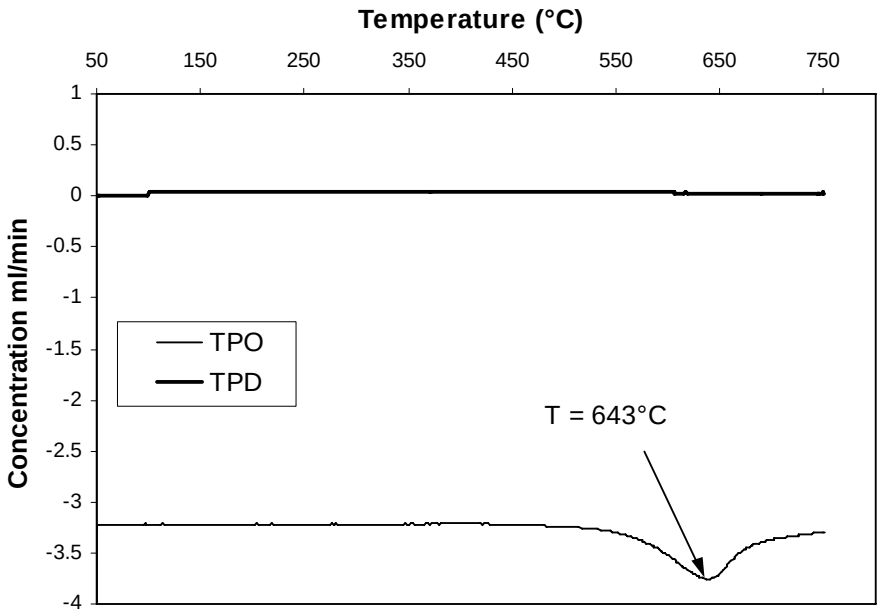

Figure 1.4. Oxygen adsorption on the cesium side during calcinations

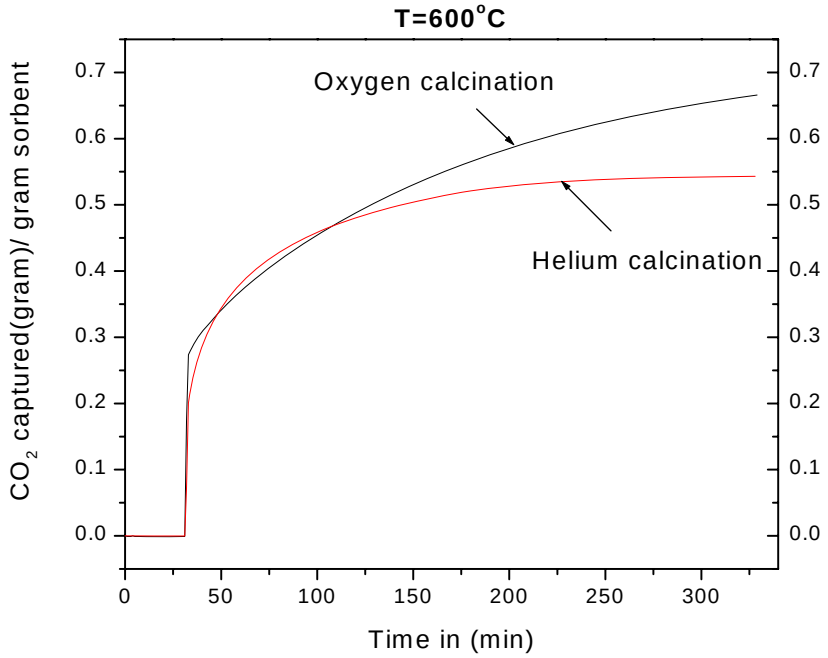

Figure 1.5. Effect of calcination gases on 20 wt% Cs/CaO; complete adsorption isotherm;

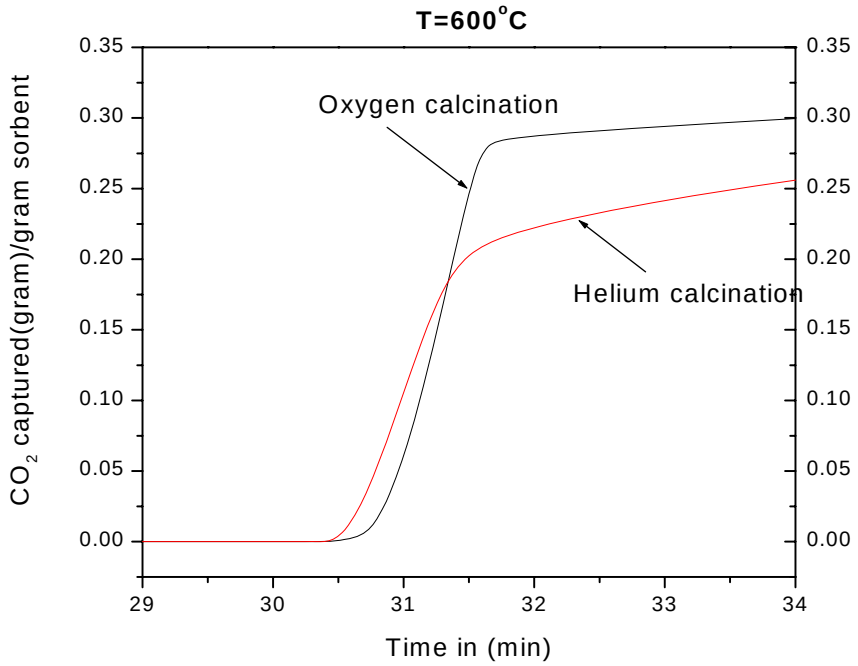

Figure 1.6. Effect of calcination gases on 20 wt% Cs/CaO; adsorption isotherm of rapid adsorption step

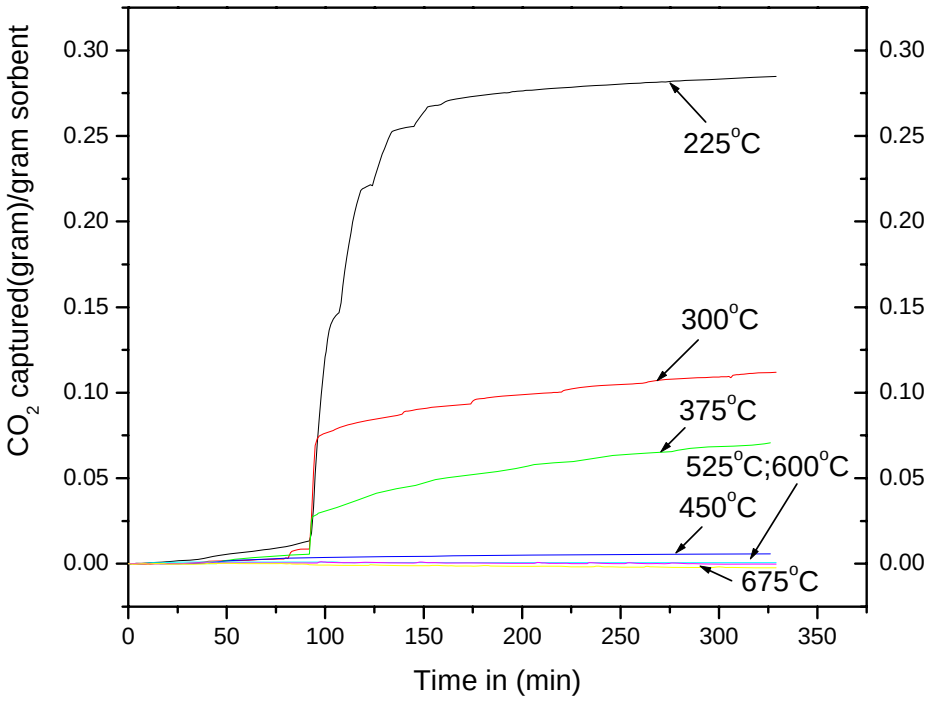

Figure 1.7. Effect of temperature for H_2O adsorption over 20 wt% Cs/CaO: concentration of H_2O = 10% balanced on helium; Total flow = 70ml/min

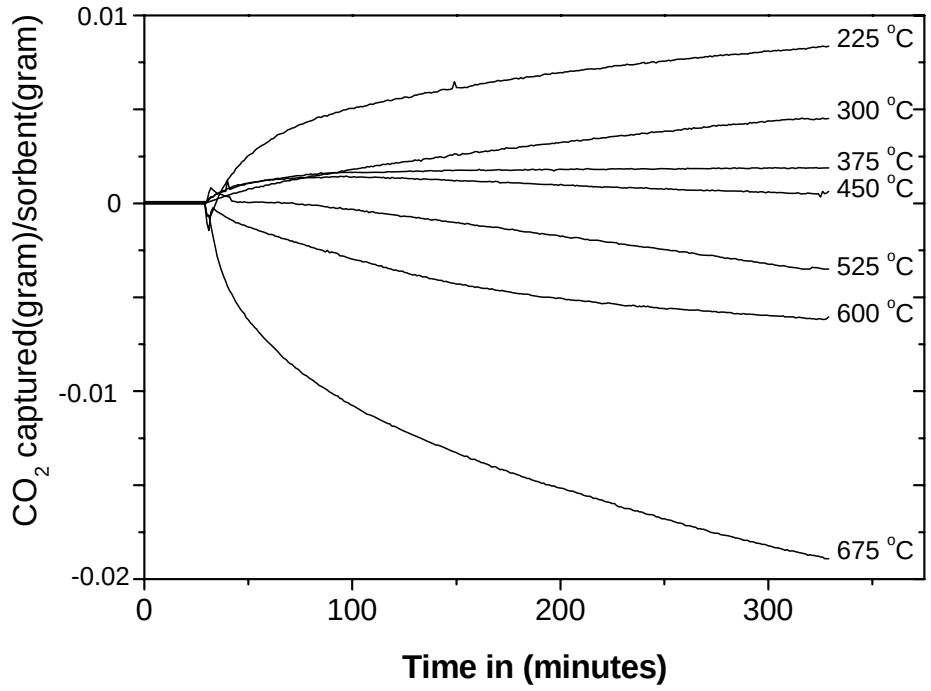

Figure 1.8. Effect of temperature for NO adsorption over 20 wt% Cs/CaO: concentration of NO = 4000ppm balanced on helium; Total flow = 70ml/min

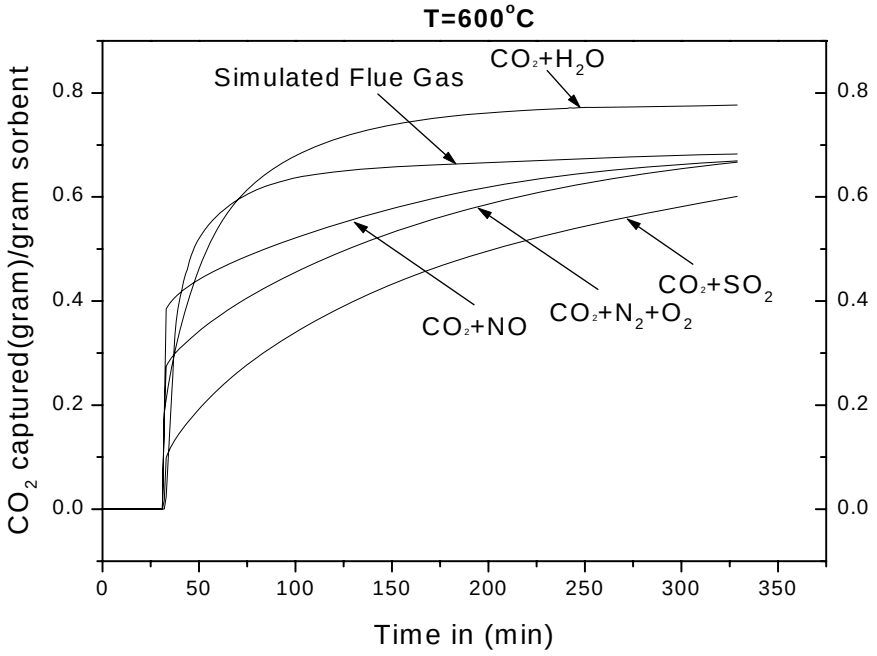

Figure 1.9. Effect of flue gas compound for CO_2 adsorption: concentrations: CO_2 = 28,6%; H_2O = 10%; NO = 500ppm; balanced on helium; Total flow = 70ml/min

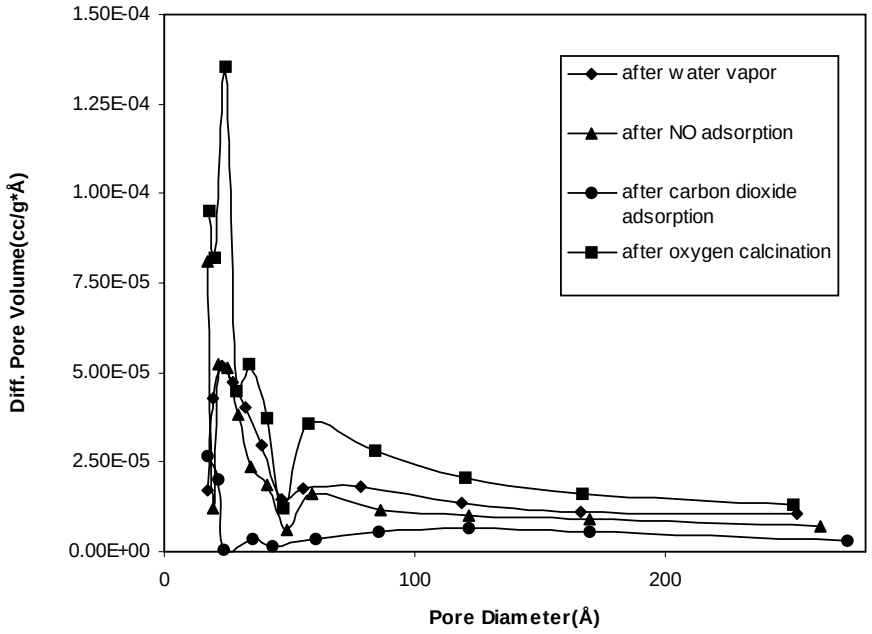

Figure 1.10. Effect of different adsorbed gases for morphological properties on 20 wt% Cs/CaO

Chapter 2. Calcium Oxide Based Sorbents for Adsorption of Carbon Dioxide at High Temperatures

Executive Summary

Five precursors were used to synthesize CO_2 sorbents in this work. CaO sorbents prepared from calcium acetate monohydrate were identified as the best candidate for the adsorption of CO_2. In a wide operation window of 550-800 ^oC, this sorbent achieved a high carbonation of more than 94%. When the adsorption temperature was 700 ^oC, about 90% of the sorbent reacted with CO_2 within the first 10 min of the carbonation. The $CaAc_2$-CaO also showed capability of maintaining its reversibility over multi adsorption-desorptions, even under the existence of 10 vol % water vapor. In a 27 cyclic adsorption-desorption experiment, the sorbent still sustained fairly high conversion of 62%, of which the adsorptions were conducted under 30 vol% CO_2 (balanced in helium), 700 ^oC and desorptions conducted under helium, 700 ^oC. When "refractory" silica was doped on these sorbents, it didn't apparently enhance durability of the sorbent.

The performed work constitutes about 60% of the proposed work and offers a screening for effectiveness in conjunction with the most important operating parameters. Our efforts fall within the budget.

We aim at improving the durability of our sorbents moreover by pinpointing specific sorbent particle size, structure, and dopants. Our long term plans for this project will be to test the best and most durable sorbents in the presence of SO_2.

2.1. Introduction

Greenhouse gases, such as CO_2 are responsible for global warming. In order to mitigate the greenhouse impact, it's important to sequester CO_2 from stationary sources, such as flue gas from fossil fuel power plants, which account for about one third of all anthropogenic CO_2 emissions (Herzog et al, 2004). Yong et al (2002) and Aaron (2005) reviewed the separation of CO_2 from flue gas. The reversible carbonation and calcination reactions of calcium oxide with CO_2 provided a viable approach for CO_2 capture and separation from high temperature gas streams, such as flue gas, gas stream generated during coal gasification, fuel cell applications, and chemical heat pump (Gupta et al, 2002; Ida et al, 2003; Reddy et al, 2004).

Recently, researchers concentrated on how to enhance the uptake capacity and reversibility of calcium oxide sorbent. In a research attempt to apply CaO for thermal energy storage, Aihara et al (2001) synthesized a reactant of CaO and calcium titanate with molar ratio of 1:1. The molar conversion of CaO was about 60% after ten carbonation-calcination cycles. Gupta and Fan (2002) managed to achieve high CaO sorbent performance by synthesizing it from precipitated calcium carbonate which was prepared from calcium hydrate. In an effort to develop hydrogen production process, Japanese researchers enhanced the reactivity and durability of CaO sorbents by an intermediate hydration treatment during multi cycle operation. More than 85% carbonation of the sorbents was achieved after seven cyclic operations at 973 K under the partial CO_2 pressures of 6.0 or 9.0 MPa. For the sorbents which were not treated by hydration, they exhibited much lower carbonation conversions (Kuramoto and Fujimoto et al, 2003; Kuramoto and Shibano et al, 2003). Reddy and Smirniotis (2004) studied the promotion effect by doping alkali metals on CaO sorbent. They observed that uptake capacity of the sorbent was significantly enhanced when cesium was used as dopant. Moreover, it was noticed that the sorbent has zero affinity to N_2 and O_2.

The objective of this research is to develop high performance sorbents for CO_2 at high temperatures by using various calcium oxide precursors. The reversibility of sorbents will be tested at suitable reaction conditions. The effect of doping silica on sorbent performance was also studied.

2.2. Experimental

Sorbents preparation. Calcium nitrate tetra hydrate (Fisher), calcium oxide (Aldrich), calcium hydroxide (Fisher), calcium carbonate (Fisher), and calcium acetate monohydrate (Fisher) were used as calcium oxide precursor sources. Calcium oxide sorbents were synthesized by calcination of these precursors as follows. The precursor was heated from 50 ^oC to 750 ^oC with a ramp rate of 10 ^oC/min and kept at 750 ^oC for 30 min in the purpose of full calcination of precursors to calcium oxides. During the entire calcination progress, the sample was kept under helium atmosphere. In this work, the calcium oxide sorbents loaded with various weight percentages of silica were synthesized by wet impregnation method. In a typical synthesis, calcium acetate precursor which corresponds to one gram calcium oxide was added to a 100 ml beaker containing 80 ml of DI water. After the calcium acetate was completely dissolved into water under continuously stirring at 70 ^oC, the appropriate amount of silica (based on silica and calcium oxide only) to result in doping levels ranging from 10-50 wt% was then added into the calcium acetate solution. The mixture was then kept under vigorous stirring at 70 ^oC until the slurry evaporated to dryness. The product was then ground to fine powder and calcined to SiO_2/CaO with the same calcination procedure as that described previously.

Characterizations. X-ray diffraction (XRD) measurements were employed for the identification of phases of the synthesized calcium oxide sorbents. The XRD patterns were conducted on a Siemens D500 powder X-Ray diffractometer with a CuK_{α} radiation source (wavelength 1.5406 Å). Aluminum holder was used to support the samples in the XRD measurements.

BET surface area and pore size distribution measurements were performed by using nitrogen adsorption and desorption isotherms at -196 ^{o}C on a Micromeritics ASAP 2010 volumetric adsorption analyzer. The calcium oxide sorbents were degassed at 300 °C for at least three hours in the degassing port of the apparatus before the actual measurement. The adsorption isotherms of nitrogen for BET measurement were collected at -196 ^{o}C by using six values of pressure ranging from about 30 mmHg to 186 mmHg. The pore size distribution measurements were obtained based on BJH method.

Particle-size distribution measurements of the sorbent material were performed with a laser scattering particle distribution analyzer (Malvern Mastersizer S series) and a Malvern dispersion unit controller. Prior to the measurements, the sorbents were subjected to ultrasound treatment.

Scanning electron microscopy (SEM) measurements were done on selected samples to get information of morphology by using a Hitachi S-400 field emission SEM. For a typical sample preparation, 5 mg of the sorbent was added into a plastic bottle which contains 20 ml of methanol. This bottle was then subject to ultrasonic treatment for 20 min. After this treatment, 1–2 drops of this suspension were transferred to the SEM sample holder and dried overnight.

Adsorption-desorption. Adsorption-desorption (carbonation-calcination) experiments were conducted with a Perkin-Elmer Pyris™-1 thermogravimertic analyzer (TGA), a Perkin Elmer thermal analysis gas station (TFGS) and the software of Pyris™ v3.8 from Perkin Elmer. The microbalance of the Pyris™-1 TGA operates as a high gain electromechanical servo system which permits detection of weight changes versus time as small as 0.1 μg. To maintain the TGA balance accurate, the helium flow of 45 ml/min was used as balance purge gas to flow over the sample. The TFGS has four gas channels and can automatically switch on either of them to introduce gas over the sample according to the reaction program. The shift between carbon dioxide and helium together with flows of them was accurately maintained by the FTGS and the reaction program.

All experiments of the adsorption and desorption, including heating the sample, cooling the sample, and shifting gases between CO_2 (99.5%, Wright Bros, Inc.) and helium were programmable and operated batch wise. A small amount of sorbent (weight ranging from 5 to 10 mg) was put in a platinum sample pan and heated to the adsorption temperature at a ramp rate of 10 ^{o}C/min. Once the sample reached the adsorption temperature, the program was automatically switched to adsorption process. After one minute the adsorption progress began, 20 ml/min of the reactant gas CO_2 was automatically switched into the system to alternate the 20 ml/min of sheath helium. When the adsorption process completed, the temperature was increased at a ramp ratio of 10 ^{o}C/min or decreased at 15 ^{o}C/min to the programmed desorption temperature. After one minute the adsorption progress completed, the 20 ml/min of CO_2 was replaced by the 20 ml/min of helium. When the desorption process finished, the temperature was increased at a ramp ratio of 10 ^{o}C/min or decreased at 15 ^{o}C/min to the adsorption temperature. A new adsorption cycle began when the temperature was achieved. In this work, typical adsorption time was set as 300 min in order to get relatively high uptake capacity of CO_2, and desorption time set

as 30 min to let the sorbent to be calcinated completely. The desorption time was intentionally kept that short to prevent possible sintering effect of sorbents. During an entire process, the sorbent weight together with the temperature was continuously recorded.

2.3. Results and discussion.

Calcium oxide sorbents were prepared by calcining various commercially available precursors, namely calcium acetate monohydrate, calcium carbonate, calcium hydroxide, calcium oxide, and calcium nitrate tetra hydrate. For simplicity, they were denoted as $CaAc_2$-CaO, $CaCO_3$-CaO, $Ca(OH)_2$-CaO, Aldrich-CaO, and $Ca(NO_3)_2$-CaO. XRD patterns of these sorbents show that they have the same peaks locating at 2 θ of 32.4, 37.6, and 54.2 degrees (Figure 2.1) which are characteristic ones of calcium oxide. This indicates that the chemical composition and physical crystallinity of all these calcium oxide sorbents prepared from different precursors are similar. They might not be the cause for different adsorption and desorption behaviors which will be discussed later.

Characteristic TGA curves of isothermal carbon dioxide adsorption over these sorbents in a 5-hour-adsorption process at 600 ^oC are presented in Figure 2.2. Chemistry schemes of calcium oxide carbonation (adsorption) and calcination (desorption) of CO_2 over CaO sorbents are described as follows:

Carbonation (adsorption): CO_2 (g) + CaO (s) $\rightarrow$ $CaCO_3$ (s) (1)

Calcination (desorption): $CaCO_3$ (s) $\rightarrow$ CO_2 (g) + CaO (s) (2)

If CaO achieved 100% carbonation conversion by following reaction (1), one molar of CaO (56 g) should take one molar of CO_2 (44 g), which is a tremendously large value. However, the reversible reaction (2) restrains the carbonation to reach the stoichiometrical point and the physical structure restricts the carbonation reaction to achieve equilibrium during reasonable experiment time. Both of these effects limit the achievement of 100% carbonation conversion value under the experimental conditions.

To compare performance of all these calcium oxide, adsorption experiments were performed at 600 ^oC under CO_2 partial pressure of 0.3 atm. For all the five sorbents, a monotonic increase of CO_2 adsorption was observed (Figure 2.2). With the exception of $Ca(NO_3)_2$-CaO, all the other sorbents exhibited rapid carbonation rates during the initial stage which were followed by an abrupt shift to a relative slower one. During the 5-hour-adsorption process at 600 ^oC, $Ca(NO_3)_2$-CaO was carbonated only about 2.5% by CO_2. Under the same adsorption conditions, Aldrich-CaO was carbonated about 25%, $Ca(OH)_2$-CaO carbonated 63 %, $CaCO_3$-CaO carbonated 66%, and $CaAc_2$-CaO carbonated 97%, which was nearly 100% conversion. The reason that the $Ca(NO_3)_2$-CaO exhibited such a low uptake capacity of CO_2 or its carbonation rate was so slow during the experiment condition is that it possessed significantly less BET surface area than the other sorbents. For the $Ca(NO_3)_2$-CaO, the BET surface area was so small that its measurement result was even not available under our test condition (Table 2.1). We observed that the precursor $Ca(NO_3)_2 \cdot 4H2O$ melted and formed solid oxide upon calcination. However, the other precursors still existed as fine powder during and after the calcination process. The cause for the complete melting and sintering of $Ca(NO_3)_2$-CaO is that the calcium nitrate tetra hydrate has a low melting temperature of about 45 ^oC. During the calcination, the precursor melted at the very early stages and finally formed solid sorbent instead of powder. This phenomenon prevents the possible formation of pores when the precursor progressed to the calcium oxide. For the Aldrich-CaO, it still existed as fine powder after

calcination which justifies its higher CO_2 adsorption capacity than the $Ca(NO_3)_2$-CaO. However, this sorbent doesn't posses many pores and its BET surface area is fairly small (4.2 m^2/g). So, its capacity was constrained to a low value (25%). With $Ca(OH)_2$ and $CaCO_3$, porosity was formed when the precursors decomposed through releasing H_2O or CO_2 (Table 2.1 and Figure 2.3). So, $Ca(OH)_2$-CaO and $CaCO_3$-CaO had better uptake capacity than the previous two sorbents. For $CaAc_2 \cdot H_2O$, its high melting temperature (about 150 ^oC) prevented the precursor from dissolving into the water released by the hydrate itself. The dissociated water evaporated before the precursor dissolved. When this metal organic compound decomposed to calcium oxide through multi steps during calcination, large volume of pores was formed.

The curve of weight versus time in Figure 2.4 depicts progressing process of the $CaAc_2 \cdot H_2O$ to CaO. The various weight plateaus correspond with the desorption of physically adsorbed gases and water, dehydration to calcium acetate, decomposition to calcium carbonate at about 400 ^oC, and consequent decomposition to calcium oxide around 600 ^oC, respectively. This multi-step decomposition ended in the formation of meso and macro pore structure (Figure 2.3). Structure difference of the sorbents is clearly depicted by SEM images (Figure 2.5). The $CaAc_2$-CaO possesses porous, "fluffy" structure while the $Ca(OH)_2$-CaO has particles which look more compact and solid. These SEM images intuitively revealed that their different pore volumes and BET surface areas are based on their different structures, which finally decided their adsorption performances. It seems carbon dioxide diffused more easily through the "fluffy" structure than through a solid one. Since these sorbents have similar particle size range (Figure 2.6), it's reasonable to propose that the different adsorption performances were induced by their different pore structures and BET surface areas. At 600 ^oC, $CaAc_2$-CaO sorbent exhibited about 97% conversion during the 5-hour-adsorption process of CO_2, the best performance among the five precursors under investigation in this research. This performance might ascribe to its larger surface area and pore volume. In order to appreciate its performance, one should notice that 97% is a significantly high uptake of about 76 wt % CO_2 per mass sorbent.

Except that the $Ca(NO_3)_2$-CaO began the carbonation with a relative slow rate from the initial stage, the other sorbents began with a rapid reaction which was followed abruptly by a much slower one. During the slow reaction regime, the reaction slowed down because CO_2 had to diffuse through the formed $CaCO_3$ layer to reach the unreacted CaO. It's suggested that the shift of the reaction mechanism happened when the surface of sorbent was covered and small pores have been blocked by formation of nonporous carbonate product layer. This layer significantly hinders the inward diffusion of CO_2. According to our results, the ratio between the carbonation rates of the fast reaction regime to those of the slow one is about two orders. This is in accordance with the results of both Hyatt et al (1958) and Barker (1973).

Since the $CaAc_2$-CaO exhibited the best performance for adsorption of CO_2 among the other sorbents being studied, we selected it to study temperature effect on CO_2 adsorption behavior. A set of experiments was conducted at temperatures ranging from 50 to 800 ^oC (Figure 2.7). When the temperatures were equal to or less than 300 ^oC, the reaction rates were fairly slow. These slow rates indicate that the reactions are kinetically controlled at the low temperatures. When the adsorption was conducted under 400 or 500 ^oC, the carbonation curves smoothly shifted from the first regime to the second regime. This suggests that the reaction mechanism transfered from kinetic control to diffusion control or the reaction was being controlled by both mass diffusion and kinetic mechanism. When the adsorption temperatures were between 550 and 800 ^oC, conversions increased to more than 94% during the five hours

adsorption. These observations indicate that the range of 550-800 ^{o}C is a suitable wide operation window for the adsorption of CO_2 over the $CaAc_2$-CaO. Under this temperature operation window, the adsorption equilibrium isotherms of carbon dioxide over $CaAc_2$-CaO are quite large when they're compared with those under lower temperatures. It's observed that the curves evolved into plateau stage shortly after the adsorption began. More than 90% of this carbonation happens within the first 10 min of the fast reaction period (Figure 2.8). The fast carbonation might be ascribed to the large BET surface area of $CaAc_2$-CaO and the diffuse control mechanism under higher temperatures. At the initial stage, the diffusion resistance obviously didn't restrain the reaction rate much because large area of sorbent was under exposure to gas phase. This rapid rate offers a great opportunity to use calcium oxide for industrial applications.

Good reversibility is a must for sorbent applications. The $CaAc_2$-CaO was chosen to test sorbent durability. 700 ^{o}C was selected as the operation temperature for both carbonation and calcination. At 700 ^{o}C, both CaO carbonation and $CaCO_3$ calcination reacted quickly. By using the same temperature for the carbonation and calcination, the continuously heating and cooling of sorbents were avoided between cyclic operations. The calcium acetate monohydrate precursor was calcined for three hours at 700 ^{o}C under oxygen in order to get better sorbent reversibility although its adsorption ability would be slightly reduced based on the first carbonation. Figure 2.9 shows that the carbonation conversion of the $CaAc_2$-CaO sorbent remained stable, even when 10 vol % water (vapor) presented in feed gases, at 93% after ten cyclic carbonation-calcinations at 700 ^{o}C. When reaction reached 10 cycles, the CO_2 uptake capacity began to decrease slowly in the following cycles. However, after 27 cycles, the sorbent still maintained relatively high conversion (about 62%). The high conversion was ascribed to its "fluffy" structure, high BET surface area, and pore volume. The decreasing of conversion through reaction cycles might be caused by the pore blockage and collapse which induced less surface area and smaller pores. The results in Table 2.1 and Figure 2.10 showed how the BET surface area and the pore volume evolved with the progressing of cyclic adsorption-desorptions. When the reaction cycles increased, the BET surface area and pore volume of sorbent decreased. When the water vapor presented in the system, the uptake capacity decreased faster than that without vapor. It's probably due to that the water "helped" the collapse of pore structure.

Sintering effects deteriorate the uptake capacity of sorbent. However, it is significant only when operation temperature is above Tammann temperature, which is estimated as 0.52 times of the melting point temperature in K. "Refractory" dopants are expected to prevent the sorbent sintering (Aihara et al, 2001). For CaO, SiO_2, and $CaCO_3$, their melting temperatures are 3171 K, 3223 K, and 1603 K, respectively. Here, their Tammann temperatures are corresponding to 1649 K, 1676 K, 834 K, individually. Thus, sintering phenomenon of the former two compounds won't occur while the last one does do at our operation temperature (973 K). The sorbents with five different weight percentages of SiO_2, namely 10 wt %, 20 wt %, 30 wt %, 40 wt %, and 50 wt % of SiO_2 (based on CaO and SiO_2 only) were studied in this work. Figure 2.11 gives the maximum carbonation values of the pure $CaAc_2$-CaO sorbent and the $CaAc_2$-CaO doped with refractory silica at 700 ^{o}C in different cycles. However, the results revealed that the durability performances of the sorbents with silica were not better than those without dopant during the four cyclic adsorption-desorptions operation. Since $CaCO_3$, the product after carbonation does sinter at 700 ^{o}C (973 K) and sintering effect does hurt sorbent performance, we proposed that

sintering effect might not be the main factor which induces adsorption performance decaying in multi cyclic carbonations. The dominant factor that causes the deterioration of carbonation might be the closure of pores and decrease of surface area during the repetitive carbonations and calcinations. So, although SiO_2 might effectively prevent $CaCO_3$ from sintering to each other, it has little impact on the overall sorbent reversibility performance.

2.4. Conclusions

Five precursors were used to synthesize CO_2 sorbents in this work. CaO sorbents prepared from calcium acetate monohydrate were identified as the best candidate for the adsorption of CO_2. In a wide operation window of 550-800 ^oC, this sorbent achieved a high carbonation of more than 94%. When the adsorption temperature was 700 ^oC, about 90% of the sorbent reacted with CO_2 within the first 10 min of the carbonation. The $CaAc_2$-CaO also showed capability of maintaining its reversibility over multi adsorption-desorptions, even under the existence of 10 vol % water vapor. In a 27 cyclic adsorption-desorption experiment, the sorbent still sustained fairly high conversion of 62%, of which the adsorptions were conducted under 30 vol% CO_2 (balanced in helium), 700 ^oC and desorptions conducted under helium, 700 ^oC. Both rapid and high uptake capacity of CO_2, together with good regenerability observed over these sorbents, was ascribed to the high BET surface area and meso and macro porous structure. This structure might be incurred in the progress of precursor decomposing during calcinations. When "refractory" silica was doped on these sorbents, it apparently didn't enhance durability of the sorbent. This illuminates that the main factor in decaying adsorption performance is the blockage and collapse of pore structure but sorbent sintering effect in multi cyclic adsorption-desorptions.

2.5. References

Aaron, D., Separation of CO_2 from flue gas: a review. *Separation Science and Technology* **2005,** 40, 321-348.

Aihara, M.; Nagai, T.; Matsushita, J.; Negishi, Y.; Ohya, H., Development of porous solid reactant for thermal-energy storage and temperature upgrade using carbonation/decarbonation reaction. *Applied Energy* **2001,** 69, (3), 225-238.

Barker, R., The Reversibility of the Reaction $CaCO_3$=CaO+CO_2. *J Appl Chem Biotechnol* **1973,** 23, (10), 733-742.

Gupta, H.; Fan, L.-S., Carbonation/Calcination Cycle Using High Reactivity Calcium Oxide for Carbon Dioxide Separation from Flue Gas. *Industrial & Engineering Chemistry Research* **2002,** 41, (16), 4035-4042.

Hyatt, E. P.; Cutler, I. B.; Wadsworth, M. E., Calcium carbonate decomposition in carbon dioxide atmosphere. *Journal of the American Ceramic Society* **1958,** 441, 70-74.

Kuramoto, K.; Fujimoto, S.; Morita, A.; Shibano, S.; Suzuki, Y.; Hatano, H.; Shi-Ying, L.; Harada, M.; Takarada, T., Repetitive carbonation-calcination reactions of Ca-based sorbents for efficient CO_2 sorption at elevated temperatures and pressures. *Industrial and Engineering Chemistry Research* **2003,** 42, (5), 975-981.

Kuramoto, K.; Shibano, S.; Fujimoto, S.; Kimura, T.; Suzuki, Y.; Hatano, H.; Shi-Ying, L.; Harada, M.; Morishita, K.; Takarada, T., Deactivation of Ca-based sorbents by coal-derived minerals during multicycle CO_2 sorption under elevated pressure and temperature. *Industrial and Engineering Chemistry Research* **2003,** 42, (15), 3566-3570.

Reddy, E. P.; Smirniotis, P. G., High-temperature sorbents for CO_2 made of alkali metals doped on CaO supports. *Journal of Physical Chemistry B* **2004,** 108, (23), 7794-7800.

Yong, Z.; Mata, V.; Rodrigues, A. E., Adsorption of carbon dioxide at high temperature--a review. *Separation and Purification Technology* **2002,** 26, (2-3), 195 - 205.

Tables and Figures

Table 2.1. Morphological Properties of various sorbents (before and after adsorption and desorption)

Sorbents	*BET (m^2/g)*	*Pore volume (cm^3/g)*
$Ca(NO_3)_2$-CaO	n/a	n/a
Aldrich-CaO	4.2	0.02
$Ca(OH)_2$-CaO	13.9	0.15
$CaCO_3$-CaO	5.3	0.08
$CaAc_2 \cdot H_2O$-CaO	20.2	0.23
$CaAc_2 \cdot H_2O$-CaO (After 1 cyclic adsorption-desorption at 700 ^oC)	18.7	0.19
$CaAc_2 \cdot H_2O$-CaO (After 2 cyclic adsorption-desorption at 700 ^oC)	19.0	0.19
$CaAc_2 \cdot H_2O$-CaO (After 4 cyclic adsorption-desorption at 700 ^oC)	18.3	0.19
$CaAc_2 \cdot H_2O$-CaO (After 8 cyclic adsorption-desorption at 700 ^oC)	14.9	0.14

n.a: not available.

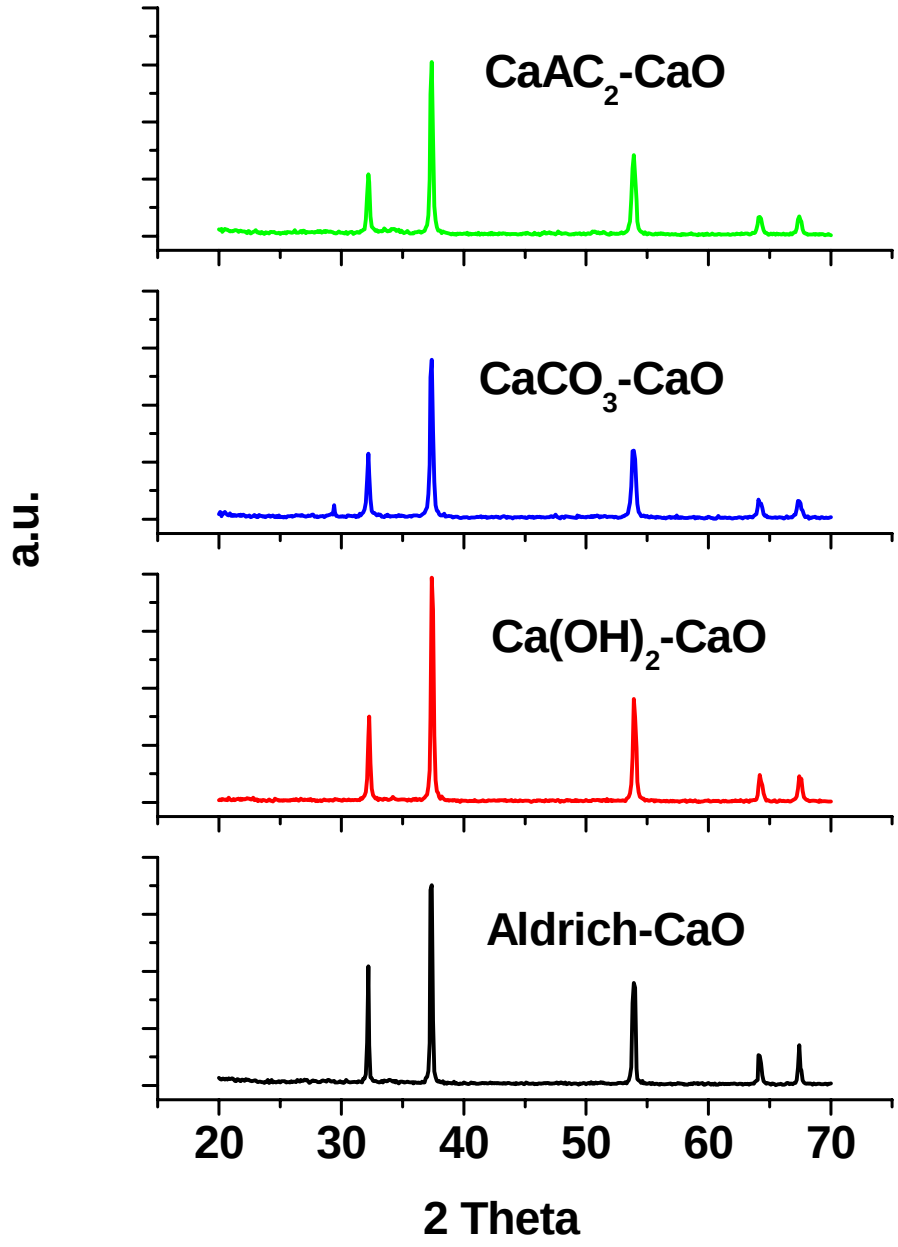

Figure 2.1. XRD patterns of calcium oxide sorbents prepared from different precursors: CaAc2·H2O, CaCO3, Ca(OH)2, and Aldrich CaO.

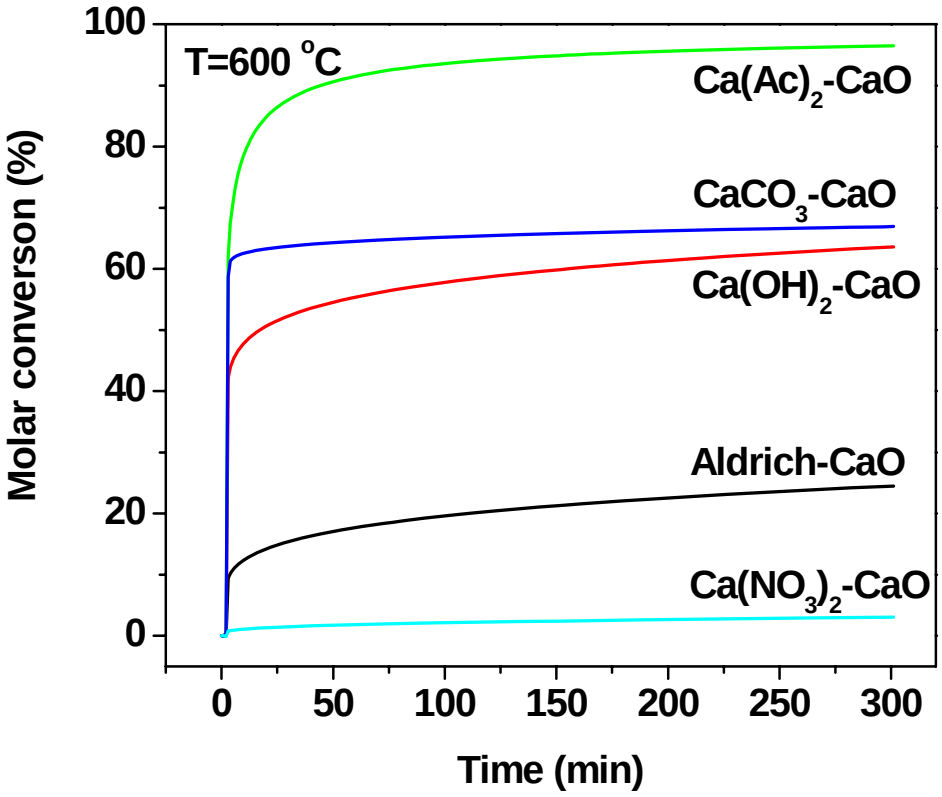

Figure 2.2. Uptake of CO_2 over CaO sorbents made with various precursors. Conditions: Temperature of adsorption, 600 ^{o}C; Concentration of CO_2, 30 vol % balanced by helium.

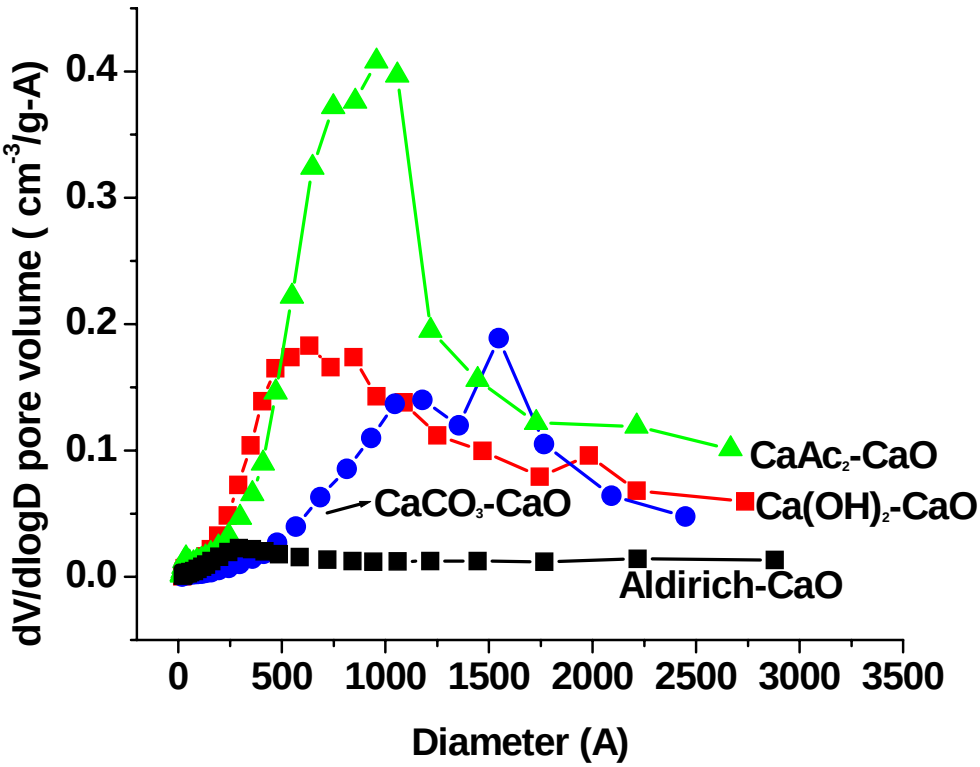

Figure 2.3. Pore size distribution of CaO sorbents prepared from CaAc2·H2O, CaCO3, Ca(OH)2, and Aldrich CaO.

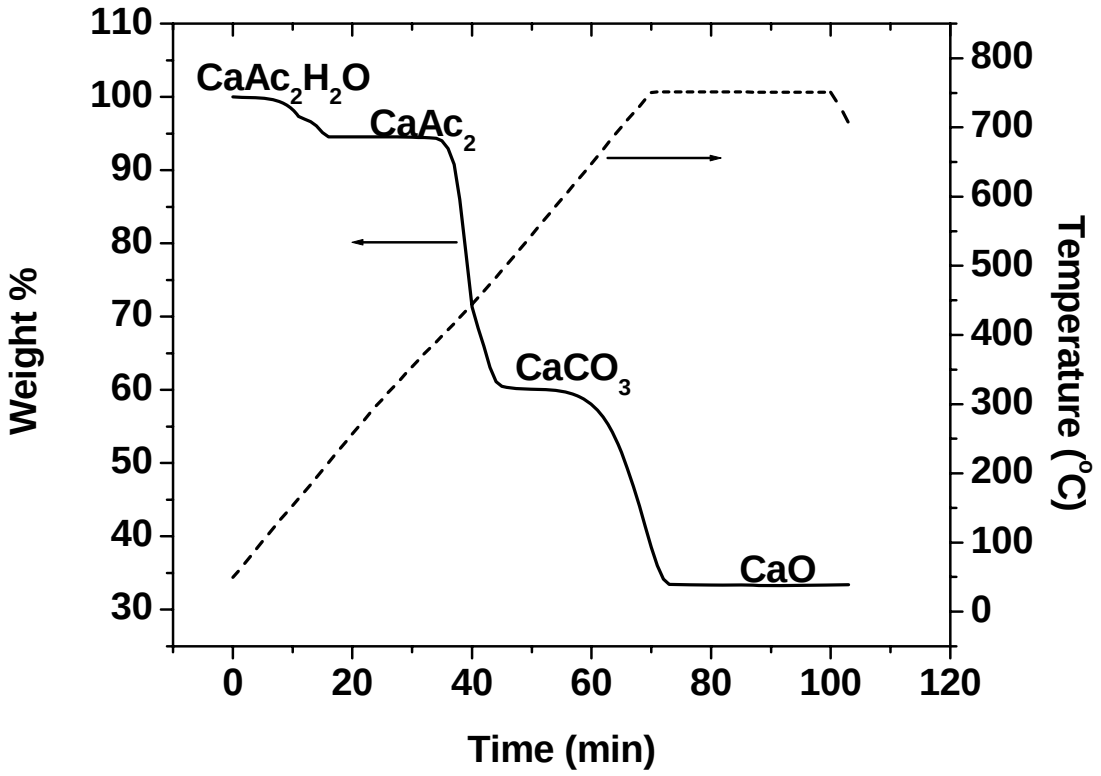

Figure 2.4. Percent weight change of $CaAc_2 \cdot H_2O$ during calcination. Conditions: Temperature ramp 10 ^{o}C/min; Atmosphere: helium.

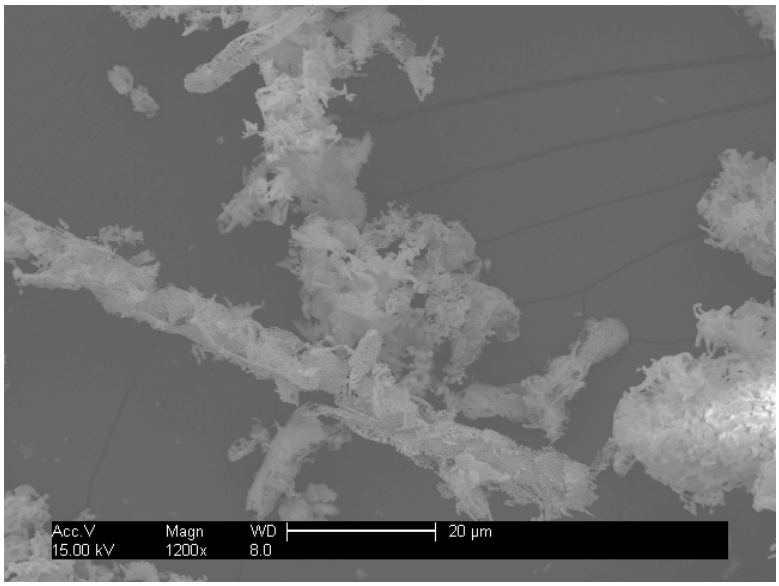

a.

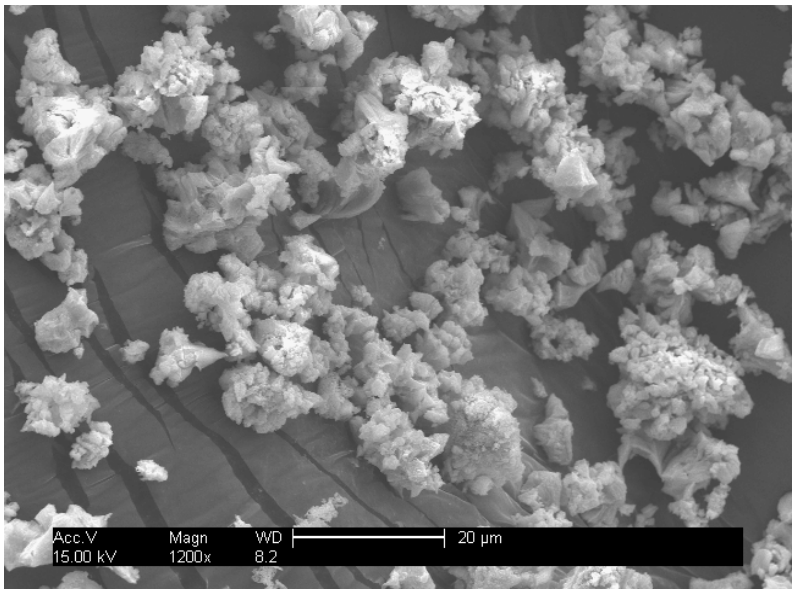

b.

Figure 2.5. SEM images of CaO sorbents: a, CaAc2·H2O-CaO; b, Ca(OH)2-CaO.

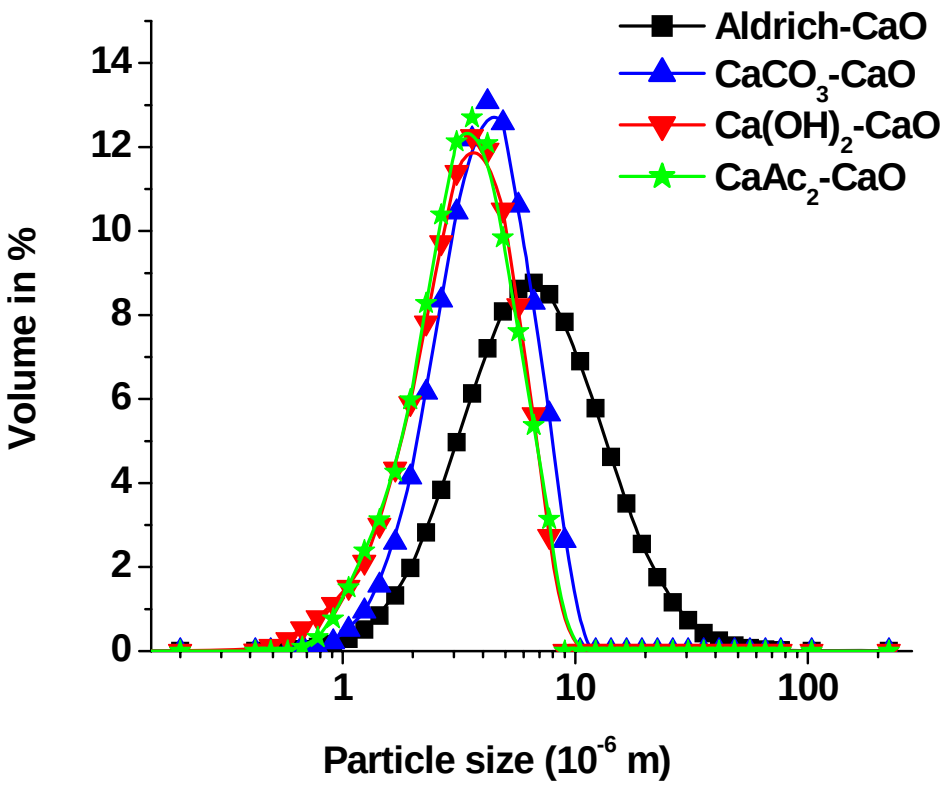

Figure 2.6. Particle size distribution of CaO sorbents prepared from CaAc2·H2O, Ca(OH)2, CaCO3, and Aldrich CaO.

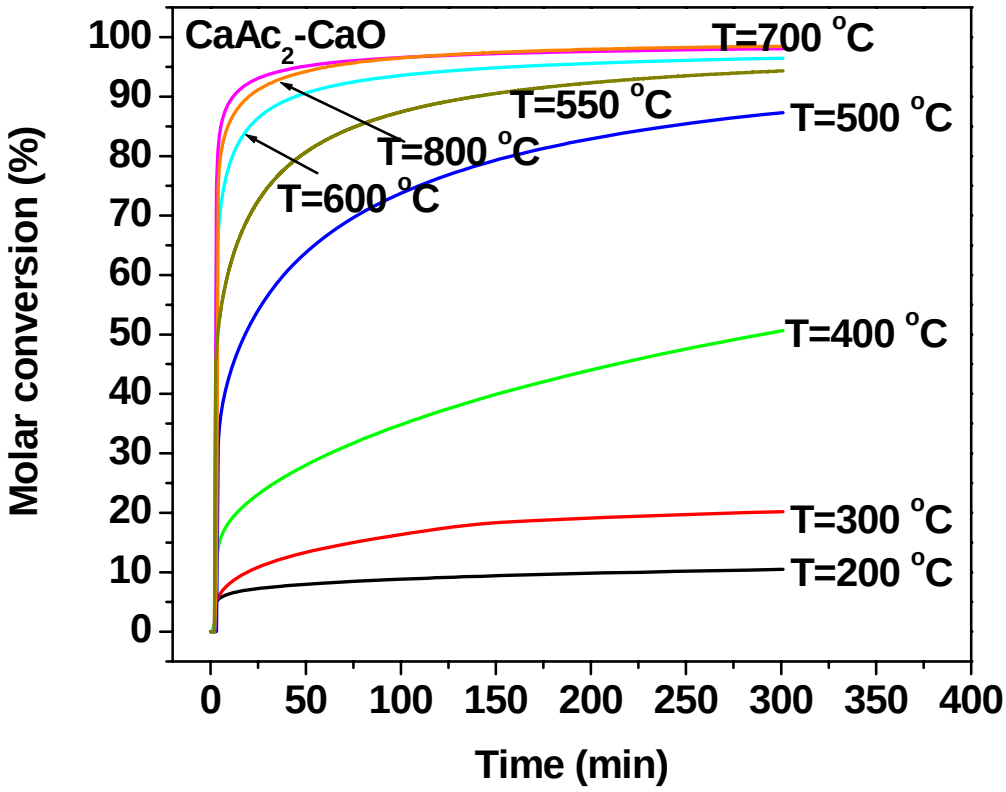

Figure 2.7. Effect of temperature on adsorption of CO_2 over $CaAc_2$-CaO. Conditions: Temperature of adsorption, 50 °C, 200 °C, 300 °C, 400 °C, 500 °C, 600 °C, 700 °C, and 800 °C; Concentration of CO_2, 30 vol % balanced by helium.

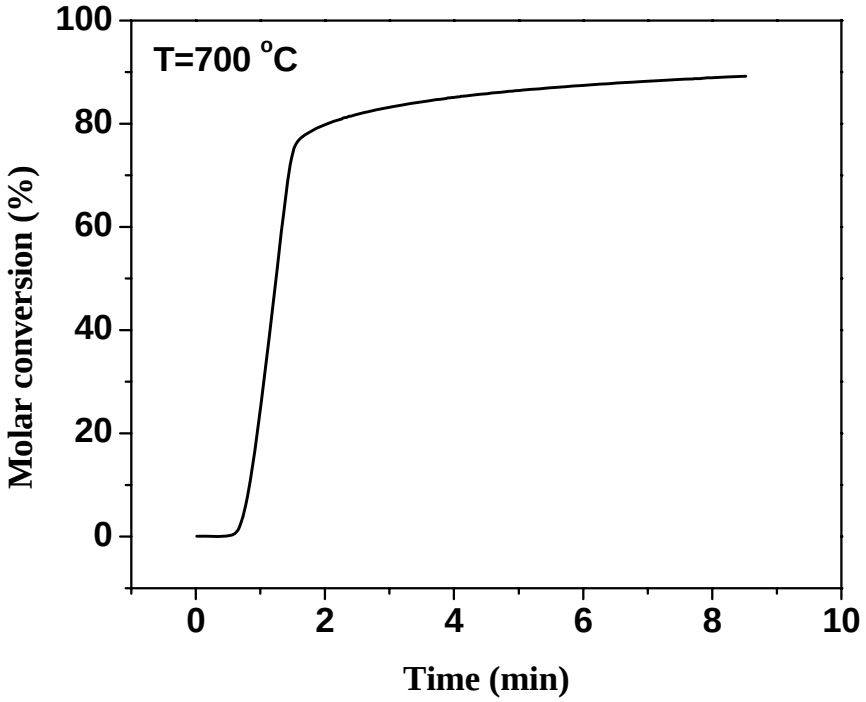

Figure 2.8. Adsorption of CO_2 over $CaAc_2$-CaO at initial stage. Conditions: Temperature of adsorption, 700 ^oC; concentration of CO_2, 30 vol % balanced by helium.

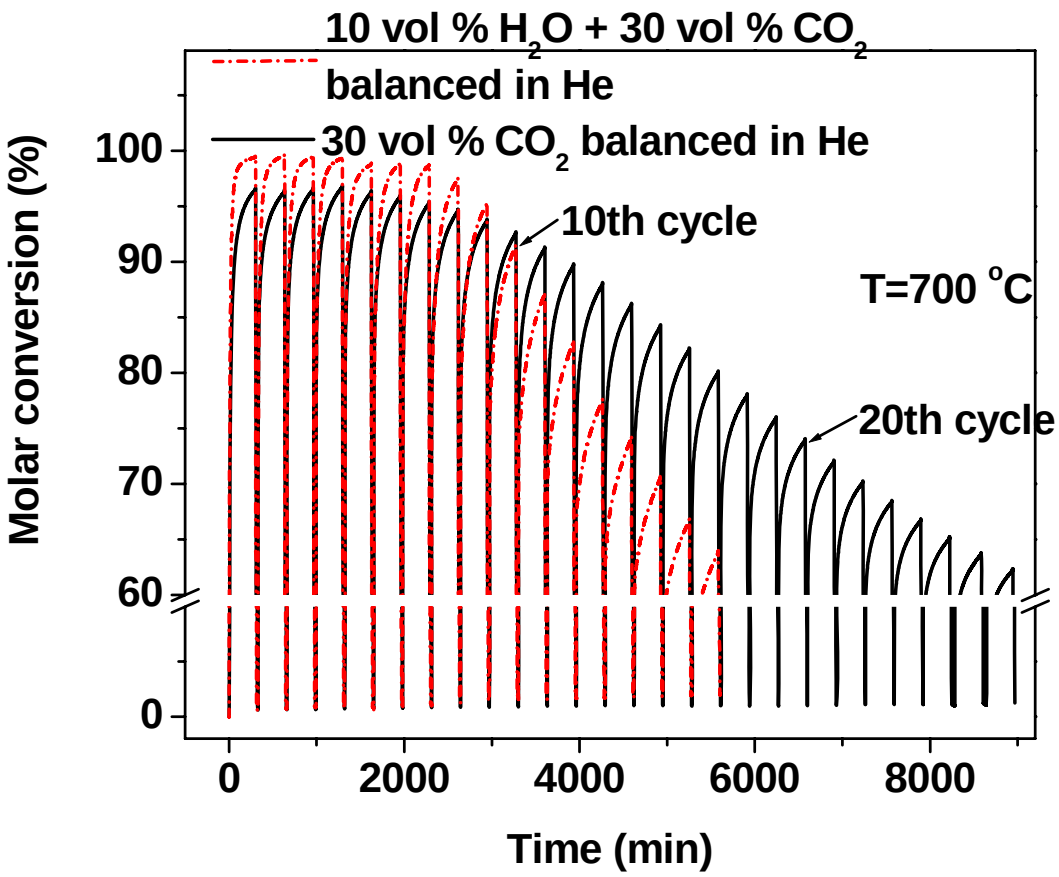

Figure 2. 9. Extended adsorption-desorption cycles of CO_2 over $CaAc_2$-CaO (27 cycles w/o water and 17 cycles w/ water). Conditions: Temperature of adsorption-desorption, 700 ^oC; Concentration of gases, a, 30 vol % CO_2 balanced by helium; b, 10 vol % H_2O (gas) + 30 vol % CO_2 balanced by helium.

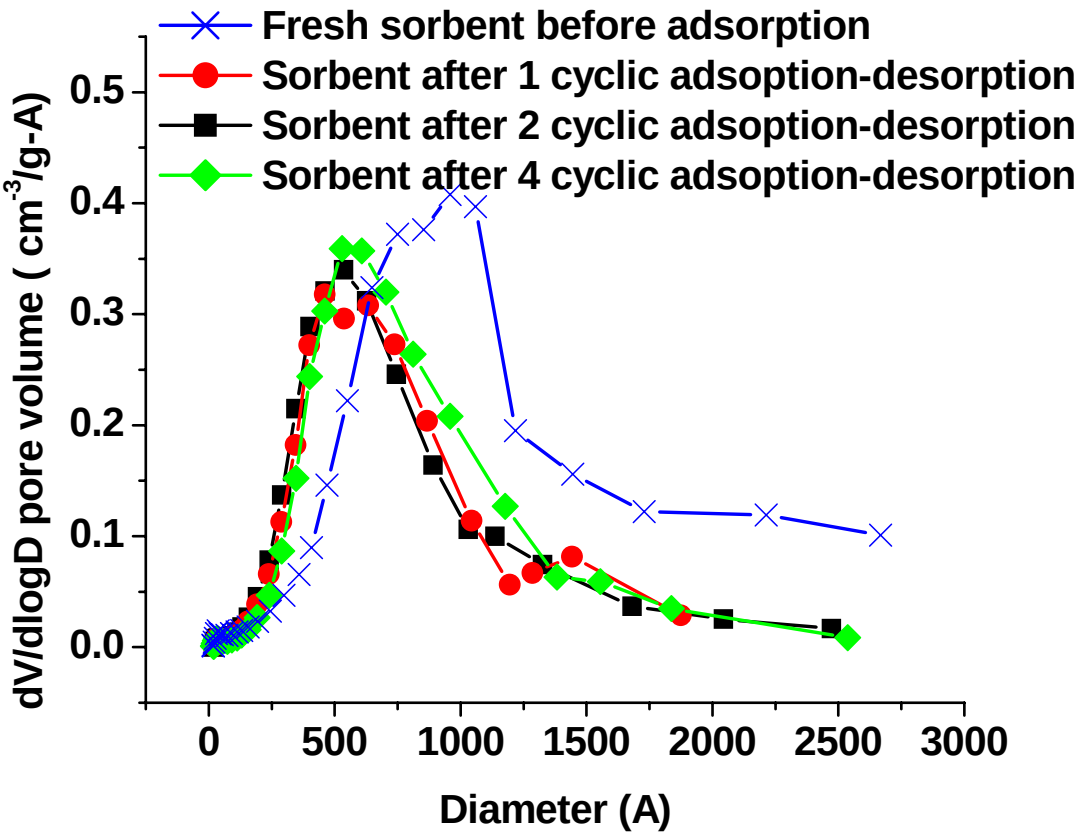

Figure 2.10. Pore size distribution of $CaAc_2$-CaO sorbents: after adsorption and desorption at 700 ^{o}C.

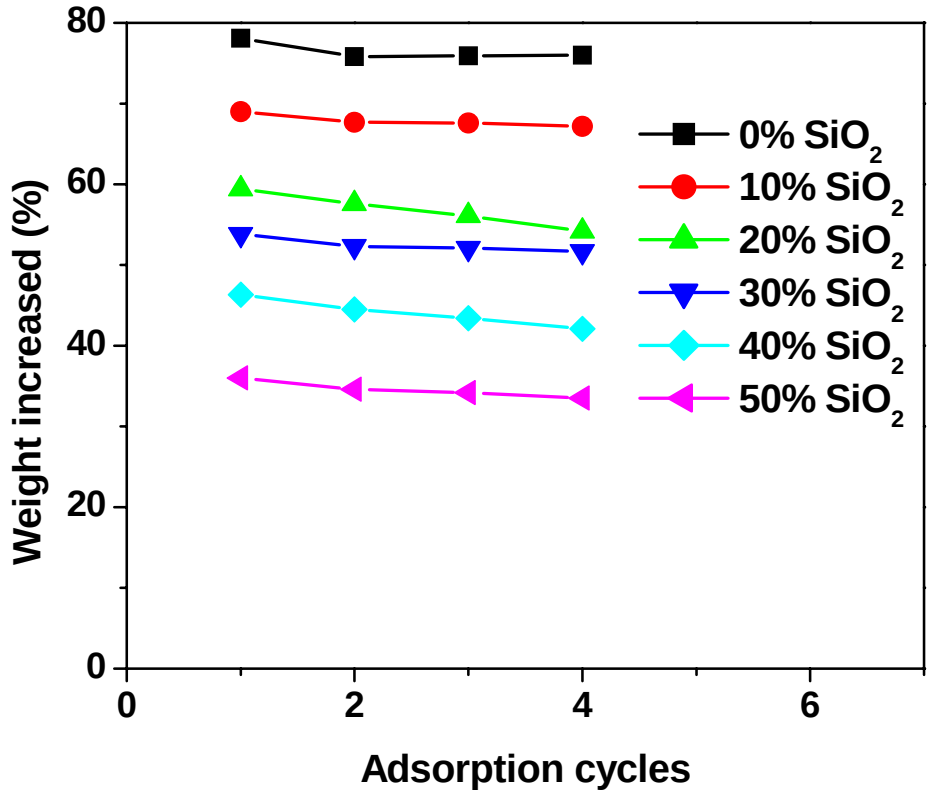

Figure 2.11. Maximum adsorption values of CO_2 over $CaAc_2$-CaO sorbents doped with 0 to 50 wt % SiO_2. Conditions: Temperature of adsorption-desorption, 700 ^oC; Concentration of CO_2, 30 vol % balanced by helium

Chapter 3. Stable Flame-Made Ca-Based Sorbents with High CO_2 Uptake Efficiency

Executive Summary

Calcium-based carbon dioxide sorbents were developed in the gas phase by flame spray pyrolysis (FSP) technique and compared to the ones made by standard high temperature calcination (HTC) of selected calcium precursors. The FSP-made sorbents were solid nanostructured particles having twice as large specific surface area (40-60 m^2/g) as the HTC-made sorbents (i.e. from calcium acetate monohydrate). All FSP-made sorbents showed high capacity for CO_2 uptake at high temperatures (773-1073 K) while the HTC-made ones from calcium acetate monohydrate ($CaAc_2 \cdot H_2O$) demonstrated the best performance for CO_2 uptake among all HTC-made sorbents. In multiple carbonation/decarbonation cycles, FSP-made sorbents demonstrated stable, reversible and high CO_2 uptake capacity sustaining maximum molar conversion at about 50% even after 60 such cycles indicating their potential for CO_2 uptake.

The performed work constitutes about 90% of the proposed work and offers a screening for effectiveness in conjunction with the most important operating parameters. Our efforts fall within the budget.

Our long term object for this project will be testing the best and most durable sorbents in the presence of vapor, SO_2, and/or at higher temperatures and less carbonation and regeneration period.

3.1. Introduction

Carbon dioxide from fossil fuel fired power plants accounts for the largest anthropogenic CO_2 emissions (1). Using metal oxide sorbents, such as calcium oxide, is one of the most potent ways to trap CO_2 and prevent its emission into the atmosphere (2-6). Gupta and Fan (3) obtained CaO sorbents from tailored porous calcium carbonate that reached 90% conversion at 973K. Salvador et al. (7) used NaCl to enhance CaO sorbents performance. Reddy and Smirniotis (5) enhanced the performance of CaO sorbents by doping alkali metals that had zero affinity to N_2 and O_2 and very low to H_2O.

While these sorbents were made largely by precipitation and/or calcination of liquid or solid Ca-precursors, an alternate route is their synthesis by gas-to-particle conversion in flames. The latter technology is a fast, cost-effective and versatile process for large scale production (several tons per hour) of carbon black, fumed silica, alumina and pigmentary titania ranging in price from $0.5 -3 /lb, depending on specifications, with no liquid byproducts (8,9). In particular, flame spray pyrolysis (FSP) allows synthesis of such particles with high specific surface areas and well defined chemical compositions, as recently demonstrated both on a lab (10) and pilot (11) scale. For example, Huber et al. (12) produced mixed $CaO/CaCO_3$ particles with BET surface areas of 31 - 103 m^2 g^{-1} for orthopedic applications by FSP of Ca-2-ethylhexanoate solutions.

Here the potential of such direct flame synthesis of calcium-based sorbents for CO_2 uptake is explored and compared to that of conventional ones made by high temperature calcination (HTC). Sorbent carbonation capacity and cycle stability are investigated at high temperatures by thermogravimetric analysis while sorbent characteristics are determined by X-ray diffraction and nitrogen adsorption.

3.2. Experimental

3.2.1. Sorbent synthesis by FSP

The experimental setup for synthesis of nanoscale powders by FSP is described in detail by Madler et al. (10). A low-cost Ca-naphthenate precursor (~35% in mineral spirits, Strem Chem., Inc.) was dissolved in xylene (Riedel-de-Haen, >96%) and fed (5 to 9 mL min^{-1}) by a syringe pump (Inotech R232) through the spray nozzle and dispersed by 3 to 5 L min^{-1} oxygen (Pan Gas, >99.95%) into fine droplets (pressure drop at the nozzle tip 1.5 bar). The resulting spray was ignited and maintained by a premixed (1.13 L min^{-1} CH_4 and 2.40 L min^{-1} O_2) flame ring surrounding the spray capillary at a radius of 6 mm (spacing was 0.15 mm) (10). Water cooling of nozzle and manifold prevents any precursor evaporation within the liquid feed lines or overheating of the nozzle. An additional oxygen sheath flow of 5 L min^{-1} was fed through a sinter metal ring (9/17 mm inner/outer diameter) surrounding the supporting flame to assure complete conversion of the reactants. The gas flows were monitored by calibrated mass flow controllers (Bronkhorst). With the aid of a vacuum pump, product particles were collected on a glass fiber filter (GF/D Whatman, 257 mm in diameter) placed in a water-cooled holder 400 mm above the nozzle, keeping the off-gas temperature below 423 K. The liquid feed rate and the dispersion oxygen flow rate were varied in order to select the product particle characteristics (13).

3.2.2 Sorbent synthesis by HTC

Calcium oxide (Aldrich), calcium carbonate (Fisher) and calcium acetate monohydrate (Fisher) were used as CaO precursors. Sorbents prepared from these three precursors by HTC are denoted as CaO-CaO, $CaCO_3$-CaO, and $CaAc_2$-CaO. Sorbents were made by HTC as follows: Precursors were heated up from 323 K to

1023 K at 10 K min^{-1} in helium and kept at 1023 K for 30 min for full calcination followed by cooling down at 15 K min^{-1}.

3.2.3. Materials characterization

The BET equivalent specific surface area (SSA) of the sorbents was determined by five-point nitrogen adsorption isotherm at 77 K in the relative pressure range of $p/p_0 = 0.05$ to 0.25 (Tristar, Micromeritics Instruments Corp.). All samples for BET measurements were degassed at 423 K for 1 h. Assuming spherical primary particles a BET equivalent particle diameter was calculated accounting for the CaO and $CaCO_3$ in sorbents, respectively, as extracted from TGA measurements in Table 3.1 while only Ca compounds were considered. The ρ_{CaO} and ρ_{CaCO3} are the bulk densities of CaO and $CaCO_3$, respectively, and SSA is the BET surface area of sorbents. Pore size distributions were obtained by nitrogen adsorption and desorption isotherms at 77 K on a Micromeritics ASAP 2010 volumetric adsorption analyzer. The sorbents for pore distribution test were degassed at 573 K for 3 h.

The crystallite sizes, d_{XRD}, were determined from x-ray diffraction (XRD) patterns recorded with a Bruker AXS D8 Advance (Cu-Kα, 40 kV, 40 mA, scanning step 0.03°, scanning time 3 s/step) by the Rietveld method with TOPAS 2 software. The powder was also analyzed by transmission electron microscopy (TEM) with a Zeiss microscope 912 Omega with ProScan and slow scan charge-coupled device (CCD) camera at 100 kV.

3.2.4. CO_2 chemisorption characterization

All carbonation/decarbonation experiments were conducted by a Perkin-Elmer Pyris™-1 thermogravimertic analyzer (TGA). This TGA was assisted by a Perkin Elmer thermal analysis gas station (TFGS) and Pyris™ v3.8 software. The TGA microbalance resolution is 0.1 μg. To maintain the TGA balance accurately, 45 mL min^{-1} of helium (prepurified, Wright Bros, Inc.) flowed over both balance and sample. The four gas channels of the TFGS can be controlled automatically to introduce reaction gas or balance inert gas into the system.

The carbonation and decarbonation experiments, including heating, cooling, and switching gases between CO_2 (99.5%, Wright Bros, Inc.) and He were programmed and operated batchwise. Sorbents (ranging from 2 to 10 mg) were placed in a platinum sample holder and heated to the desired carbonation temperature at 10 K min^{-1} under 65 mL min^{-1} flow of helium (45 mL min^{-1} purge gas and 20 mL min^{-1} balance gas). Once the sample reached the carbonation temperature, 20 mL min^{-1} helium was replaced by 20 mL min^{-1} CO_2 initiating the carbonation. The carbonation time was 60 or 300 min while the decarbonation time was always 30 min. Sorbent weight and temperature were recorded continuously throughout the experiment. Rather long reaction times were selected to test the stability of these sorbents which is a crucial characteristic for their large scale application.

3.3. Results and discussion

3.3.1. FSP-made sorbents

Nanoparticles with three different SSAs ranging from 41 to 59 m^2 g^{-1} were synthesized by FSP (Table 3.1). The BET equivalent primary particle diameters of all sorbents are 30-50 nm (Table 3.1). The XRD patters of the sorbents correspond to CaO and $CaCO_3$ as shown in Figure 3.1. High flame temperatures cause the Ca-naphthenate precursors to be initially converted into CaO particles. These particles react (partially) with combustion off-gas CO_2 in the flame tail forming $CaCO_3$. Huber et al. (12) reported that amorphous $CaCO_3$ forms in the off-gas of the flame. They also observed that slower cooling rates provide more time for particle crystallization (12).

No amorphous $CaCO_3$, however, could be identified in our sorbents as determined by the flat XRD baselines. This may be explained by different enthalpy content and shape of the present flames compared to Huber et al. (12).

Before the first carbonation, all sorbents were pretreated in helium atmosphere following the temperature profile in Figure 3.2. The initial weight percentage was set at 100%. Physically adsorbed gases and water were released first above 373 K. At 873 K, $CaCO_3$ begins to decompose into CaO. Based on the XRD results, it is reasonable to expect all Ca to be in the form of CaO or $CaCO_3$. Therefore, the composition of the sorbents can be extracted where the weight percentages of CaO and $CaCO_3$ in sorbents were obtained on the basis of equations 1 and 2:

$$w'_{CaO} + w'_{CaCO_3} = w_0 \quad (1)$$

$$w'_{CaO} + w'_{CaCO_3} * 56/100 = w_t \quad (2)$$

Where w'_{CaO} and w'_{CaCO3} are the weight percentages (Table 3.1) of CaO and $CaCO_3$ in sorbents, respectively, as obtained by initial TGA pretreatment. The w_0 is the combined weight percentage of CaO and $CaCO_3$ in the sorbents before pretreatment, and w_t is the weight percentage of CaO in the sorbent after pretreatment. Table 3.1 illustrates that there is more $CaCO_3$ than CaO in the FSP-made sorbents. These compositions are within 3% of the ones determined by XRD.

3.3.2. Carbonation/decarbonation of FSP-made sorbents

Figure 3.3 shows typical CO_2 uptake performance of the FSP sorbents in the form of molar conversion as a function of time for four carbonation/decarbonation cycles at 973 K. The samples were pretreated at 1023 K under helium for 30 min and back reacted at 973 K with CO_2. All the curves show monotonic increase of the sorbent conversion versus time during the carbonation period. Fast and complete decomposition of the carbonated $CaCO_3$ back to CaO was observed during the decarbonation period indicating reversible carbonation/decarbonation. The carbonation curves of all sorbents exhibit two stages: In the initial stage of each carbonation period, conversion increased steeply followed by a plateau in the second stage. During the four cycle operation, sorbents exhibited stable and reversible behavior, and high capacity of more than 90% molar conversion. Samples FSP1 and FSP2 behaved similarly while FSP3 with the highest SSA (Table 3.1) showed the highest capacity and uptake rate as extracted from the steep slope in the first stage. Apparently the high performances are ascribed tothe high SSAs.

Figure 3.4 shows maximum sorbent carbonation conversion achieved at each carbonation period as a function of the number of cycles for flame-made sorbents. The carbonation time was 60 min. In the first 10 carbonation cycles, their capacities remained quite stable and reversible. In the following cycles, the CO_2 uptake capability decreased while for operation beyond about 40 cycles the performance became quite stable again. Decreasing carbonation/decarbonation time would actually make the sorbent performance even more “stable” as sintering effects would be mitigated during shorter reaction period (Results not shown). The overall performance is comparable for all three sorbents although FSP3 with the highest SSA shows initially higher conversion and slightly lower at later cycles. The deterioration in sorbents’ performance is induced by sintering as indicated from sorbent TEM images (Figure 3.5a, c). Figure 3.5c shows typical FSP-made sorbent particles after one cycle operation. The particles were sintered and became much larger - decreasing their SSA - than before interaction with CO_2 (Figure 3.5a). High SSA particles are more prone to sintering explaining the stronger deterioration of sample FSP3. The initial SSA of the sorbents did not affect their performance in cyclic operation (50 cycles).

Following pretreatment, the Ca of all sorbents existed only in the form of CaO regardless of the initial $CaCO_3$ content. It's worth noting that the flame-made sorbents demonstrated similar performance although they contained quite different percentages of CaO and $CaCO_3$ before pretreatment. Therefore, the original percentages of CaO and $CaCO_3$ in the sorbents did not play significant role in their carbonation performance.

3.3.3. Sorbents made by HTC

Three sorbents were prepared by calcining CaO, $CaCO_3$, and $CaAc_2$ at 1023 K. Their capability to capture CO_2 at 773 K and 973 K are presented in Figure 3.6. All three sorbents demonstrated much higher uptakes at 973 K than at 773 K. The conversion of CaO-CaO increased the most and that of $CaAc_2$-CaO the least from 773 K to 973 K. The $CaAc_2$-CaO, exhibited the highest capacity for CO_2 uptake than the other two sorbents. Its conversion even at 773 K is much higher than that of the others at 973 K. Table 3.2 and Figure 3.7 suggest that the high performance of $CaAc_2$-CaO sorbents is related to their large BET surface area and pore volume. The pore volume of the $CaAc_2$-CaO is as large as 0.23 $cm^3\ g^{-1}$, which is eleven times larger than that of CaO-CaO, and nearly four times larger than $CaCO_3$-CaO. Figure 3.7 shows pore size distributions of the three HTC samples. The $CaAc_2$-CaO sorbents have not only much larger pore volumes (Table 3. 2) but also narrower pore size distribution than the other HTC sorbents. Thermogravimetric analysis (Figure 3.8) revealed multiple precursor decompositions till the final CaO sorbent porous structure as below:

$$Ca(CH_3COO)_2\cdot H_2O \xrightarrow{>\sim 400\ K} Ca(CH_3COO)_2 \xrightarrow{>\sim 680\ K} CaCO_3 \xrightarrow{>\sim 900\ K} CaO$$

3.3.4. Comparison of FSP- and HTC-made sorbents

FSP-made sorbents contained more $CaCO_3$ than CaO. Thus, carbonation of FSP-made sorbents was compared to HTC-made sorbents from commercial $CaCO_3$. Figure 3. 9 shows the molar conversion as a function of time for FSP3-CaO and HTC $CaCO_3$-CaO at 973 K. Both sorbents show similar kinetic behavior during the first stage of carbonation. However, the FSP-made sorbent exhibited much higher capacity during the five-hour-carbonation with CO_2. Comparing Tables 3.1 and 3.2 shows that the SSAs of FSP-made sorbents are about one order of magnitude larger than those of the $CaCO_3$-CaO sorbents. After the surface CaO was consumed during carbonation, CO_2 had to diffuse through a shell of solid $CaCO_3$ to reach the internal unreacted CaO. Therefore, the $CaCO_3$-CaO sorbents offered much larger resistance for CO_2 transfer and presented less capacity than the FSP-made sorbents during a five-hour-carbonation.

Figure 3.5b shows typical TEM images of HTC $CaCO_3$-CaO. The primary particle sizes of the FSP-made sorbents (Figure 3. 5a) are between 30 and 50 nm consistent with their BET equivalent diameter (Table 3.1). This indicates that, by assuming the sorbent particle to be spheres, the particle sizes acquired from SSAs are reliable. For $CaCO_3$-CaO particles, a BET equivalent particle diameter in the range of 400 nm would be expected which is not supported by our TEM observations. Indeed $CaCO_3$-CaO particles look more compact (Figure 3. 5b) and sintered. The representative images of particles of both FSP-made and $CaCO_3$-CaO sorbents, respectively, demonstrate that sintering did happen among the particles for both sorbents after one cyclic carbonation/decarbonation at 973 K (Figure 3. 5c, d).

Both FSP-made and $CaAc_2$-CaO sorbents revealed high capacity for CO_2 uptake because of the large SSA arising from their nanostructure and porous structure, respectively. Figure 3. 10 shows the CO_2 uptake of both sorbents from 323 K to

1073 K. Below 773 K, FSP-made sorbents demonstrated better performance because of their larger SSA. Above 773 K, however, $CaAc_2$-CaO sorbents showed higher conversion implying that larger SSA (>20 m^2 g^{-1}) may offer advantages for CO_2 uptake up to a certain temperature only. This may be explained by sintering of sorbent with higher SSA. At high temperatures, the carbonation rate is limited by the product layer diffusion. When both sorbents have large SSA, sorbent morphology will have important impact on the transfer of reaction gas to the sorbent surface, something that may influence the overall carbonation rate.

3.3.5. Stability of FSP-made sorbents and $CaAc_2$-CaO made by HTC

For CO_2 uptake by the sorbent, stability is more important than capacity. Both the FSP-made and HTC-made from $CaAc_2$-CaO sorbents have high capacity for CO_2 uptake at high temperatures. Here 973 K was chosen as both carbonation and decarbonation temperature. At 973 K, a) the sorbents carbonated fast, could reach higher conversion or regenerate completely back to CaO relatively quickly; b) repetitive heating and cooling ramp were avoided between cyclic operations by using the same temperatures for carbonation and decarbonation. It should be noted that these temperatures are lower than the ones used for sorbents made from lime/limestone, a distinctive advantage of the present nanostructured flame-made sorbents.

Figure 3.11 presents the maximum molar conversion of the sorbents during 300 min carbonation period as a function of carbonation/decarbonation cycles. During the initial cycles, both sorbents could keep their high conversion in the range of about 95%. After that point, the performance of both sorbents began to decrease. The capacity of the $CaAc_2$-CaO decreased almost linearly with respect to the cycles of operation while that of FSP-made ones decreased faster. After about 20 cycles, however, the maximum conversion of the FSP-made sorbents remained around 50% for the following 40 cycles. This is substantially higher than the 20% after just 20 carbonation/decarbonation cycles reported in the literature (14). Note that sorbents and experimental conditions employed among these data are different. Our sorbents underwent decarbonation at relatively lower temperature (973 K).

3.4. Conclusions

Ca-based sorbents made in flames demonstrated excellent performance for CO_2 uptake at high temperatures (773 – 1073 K). This was attributed to their high specific surface area (40-60 m2/g), a characteristic of nanostructured particles. When calcium acetate monohydrate was used as calcination precursor, calcium sorbents also exhibited high performance at the initial carbonation/decarbonation cycles. After about 10 cycles the performance of the latter sorbents decreased almost linearly with increasing cycles. The FSP-made sorbents, however, presented stable, reversible maximum molar conversion around 50% during 60 cycles of operation.

"Refractory" silica, titania, and zirconia were doped on these sorbents by flame technique, sorbents with zirconia exhibit better stability than other sorbents. Among sorbents doping with zirconia, the one having a ratio of 3:10 between Zr to Ca shows stable performance during 102-cycle operation. This stable performance should be ascribed to the refractory zirconia preventing possible particle sintering and structure collapse during reaction. The mechanism behind these is still under investigation.

3.5. References

(1) Herzog, H.; Gollomb, D. *Encyclopedia of Energy*; Elsevier Science Inc.: New York, **2004**.

(2) Silaban, A.; Harrison, D. P. High temperature capture of carbon dioxide: characteristics of the reversible reaction between CaO(s) and CO_2(g). *Chem. Eng. Comm.* **1995**, 137, 177-190.

(3) Gupta, H.; Fan, L.-S. Carbonation/calcination cycle using high reactivity calcium oxide for carbon dioxide separation from flue gas. *Ind. & Eng. Chem. Res*. **2002**, *41*, 4035-4042.

(4) Ida, J.-I.; Lin, Y. S. Mechanism of high-temperature CO_2 sorption on lithium zirconate. *Environ. Sci. Technol*. **2003**, *37*, 1999-2004.

(5) Reddy, E. P.; Smirniotis, P. G. High-temperature sorbents for CO_2 made of alkali metals doped on CaO supports. *J. Phys. Chem. B*. **2004**, *108*, 7794-7800.

(6) Alvarez, D.; Abanades, J. C. Pore-size and shape effects on the recarbonation performance of calcium oxide submitted to repeated calcination/recarbonation cycles. *Energ. & Fuels*. **2005**, *19*, 270-278.

(7) Salvador, C.; Lu, D.; Anthony, E. J.; Abanades, J. C. Enhancement of CaO for CO_2 capture in an FBC environment. *Chem. Eng. J*. **2003**, *96*, 187-195.

(8) Pratsinis, S. E. Flame aerosol synthesis of ceramic powders. *Prog. Energ. Combust. Sci*. **1998**, *24*, 197-219.

(9) Wooldridge, M. S. Gas-phase combustion synthesis of particles. *Prog. Energ. Combust. Sci*. **1998**, *24*, 63-87.

(10) Madler, L.; Stark, W. J.; Pratsinis, S. E. Flame-made ceria nanoparticles. *J. Mater. Res*. **2002**, *17*, 1356-1362.

(11) Mueller, R.; Madler, L.; Pratsinis, S. E. Nanoparticle synthesis at high production rates by flame spray pyrolysis. *Chem. Eng. Sci*. **2003**, *58*, 1969-1976.

(12) Huber, M.; Stark, W. J.; Loher, S.; Maciejewski, M.; Krumeich, F.; Baiker, A. Flame synthesis of calcium carbonate nanoparticles. *Chem. Comm*. **2005**, *2005*, 648-650.

(13) Madler, L.; Kammler, H. K.; Mueller, R.; Pratsinis, S. E. Controlled synthesis of nanostructured particles by flame spray pyrolysis. *J. Aerosol Sci*. **2002**, *33*, 369-389.

(14) Abanades, J. C. The maximum capture efficiency of CO_2 using a carbonation/calcination cycle of CaO/$CaCO_3$. *Chem. Eng. J*. **2002**, *90*, 303-306.

Tables and Figures

Table 3.1. Synthesis conditions, BET Surface areas, particle diameters, and weight percentages of CaO and $CaCO_3$ of FSP-made sorbents.

Sorbent	Ca precursor solution feeding rate (ml min^{-1})	Dispersion O2 flow rate (L min^{-1})	BET surface area (m^2 g^{-1})	Particle diameter (nm)	CaO (wt. %)	$CaCO_3$ (wt. %)
FSP1	9	3	41	48	36	56
FSP2	7	3	47	41	43	48
FSP3	5	5	59	34	22	73

Diameters are Calculated from BET Surface Area. Weight Percentages are Derived from TGA Pretreatment Curves.

Table 3.2. BET surface areas and pore volumes of HTC-made sorbents

CaO Precursor	BET [m^2 g^{-1}]	Pore Volume [cm^3 g^{-1}]
$CaAc_2$-CaO	20	0.23
$CaCO_3$-CaO	5	0.06
CaO-CaO	4	0.02

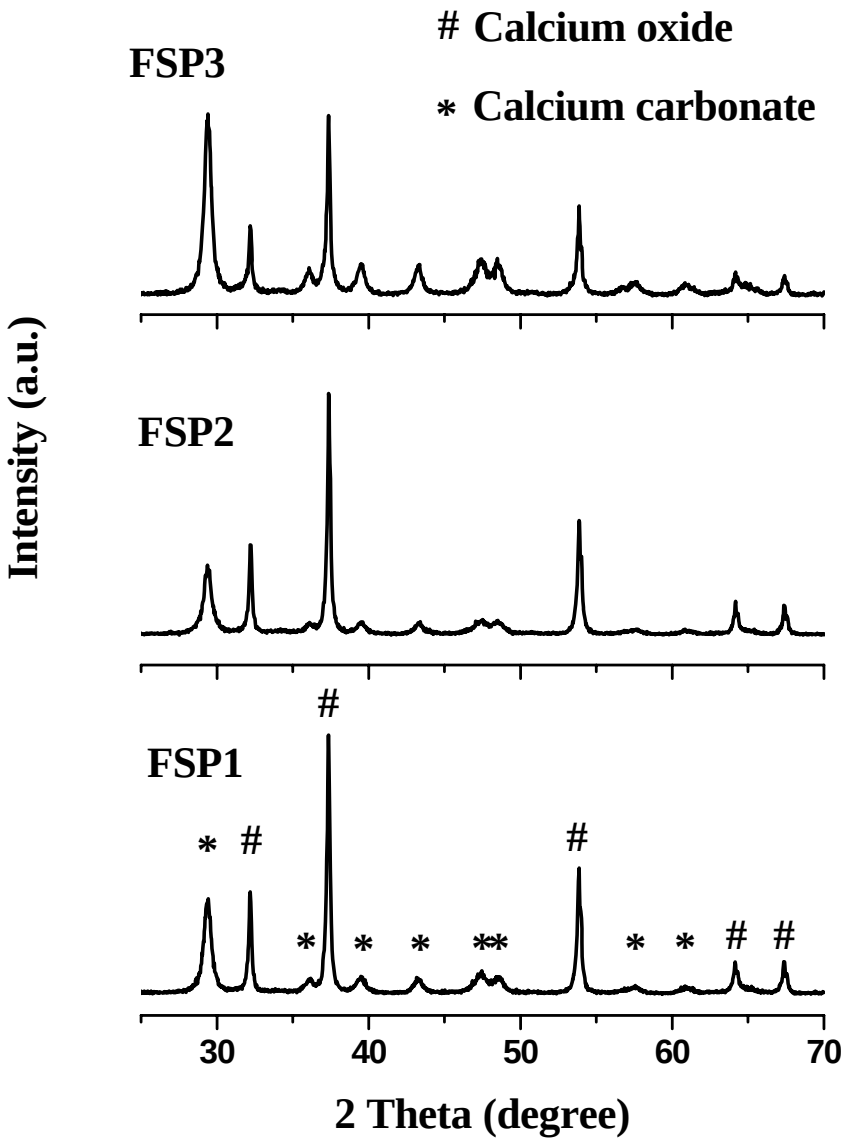

Figure 3.1. XRD patterns of as prepared FSP-made sorbents (Table 3.1). The sharp spectra and rather flat baseline indicate that these are crystalline materials.

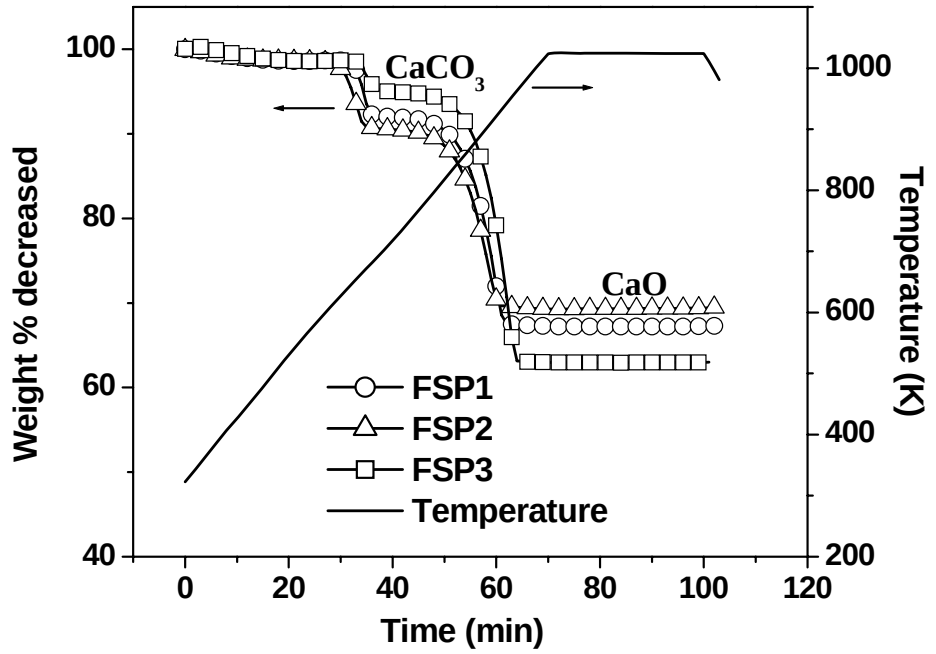

Figure 3. 2. Thermogravimetric analysis of the pretreatment of FSP-made sorbents (Table 3.1) showing the release of adsorbed H_2O (~600 K) and $CaCO_3$ (~800 K) conversion.

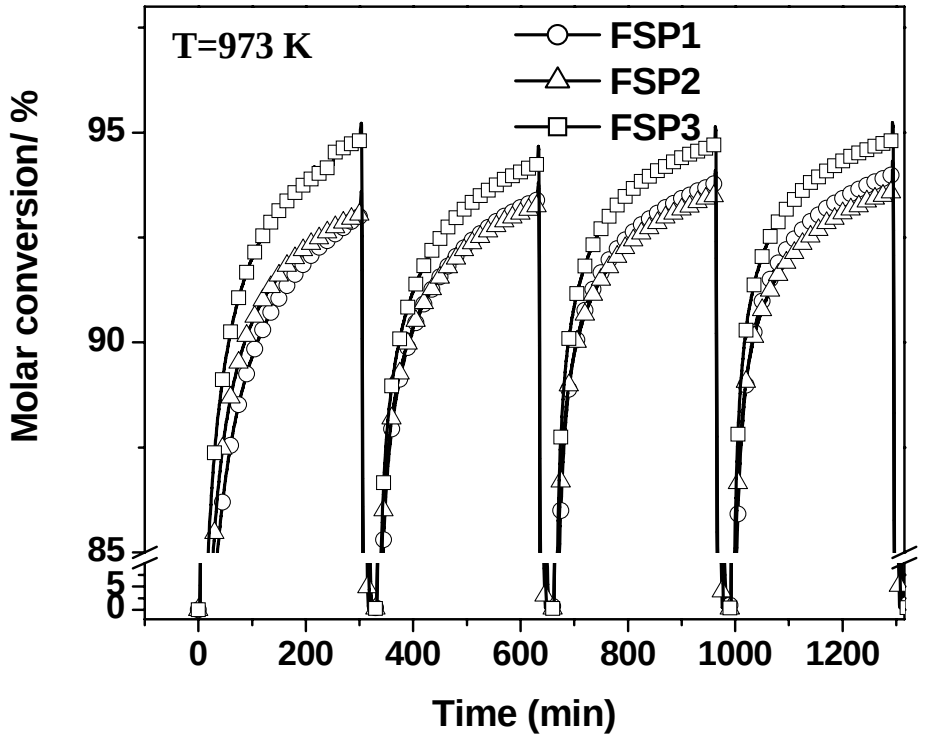

Figure 3.3. Carbonation/decarbonation cycles on FSP-made sorbents (Table 3.1) at 973 K showing high capacity and reversible reactions. Carbonation/decarbonation Time: 300 min/30 min.

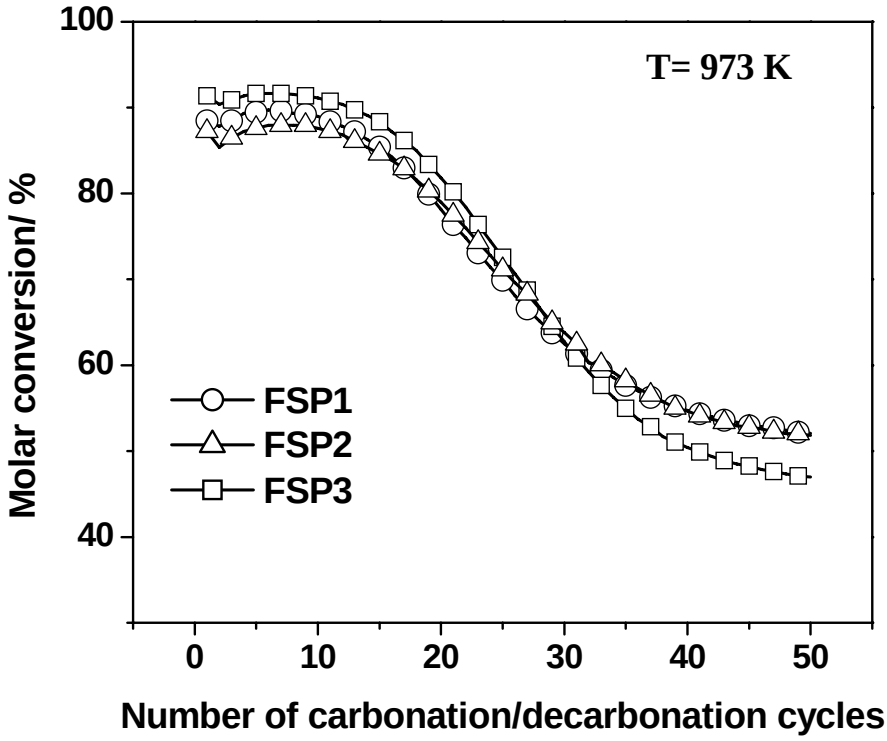

Figure 3.4. The evolution of the maximum carbonation conversion of FSP-made sorbents (Table 3.1) with the number of carbonation/decarbonation cycles (60 min /30 min) at 973 K. Stable high conversions were attained after 40 cycles.

Figure 3.5a **Figure 3.5b**

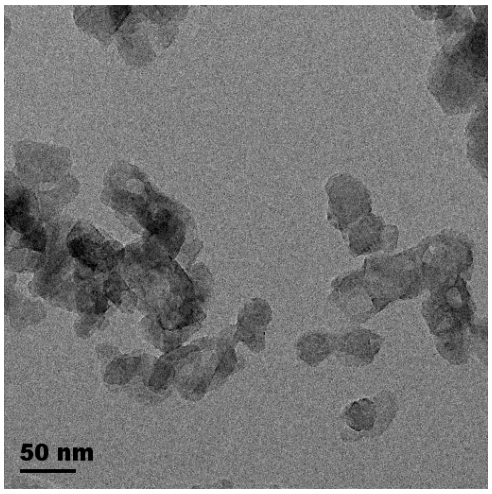

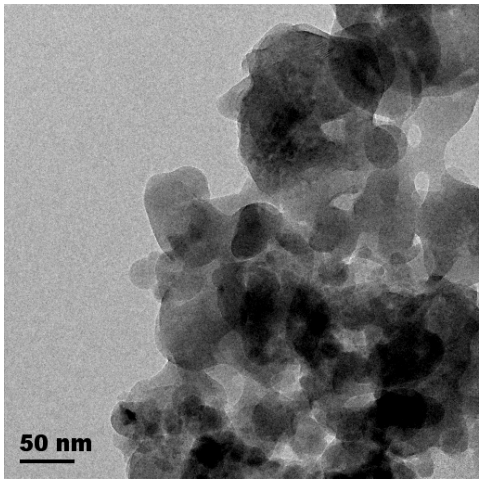

Figure 3.5c **Figure 3.5d**

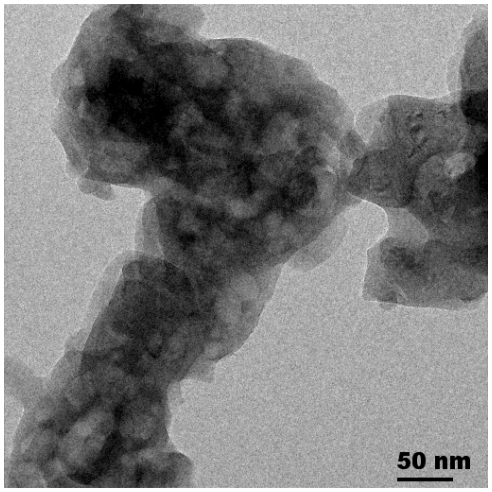

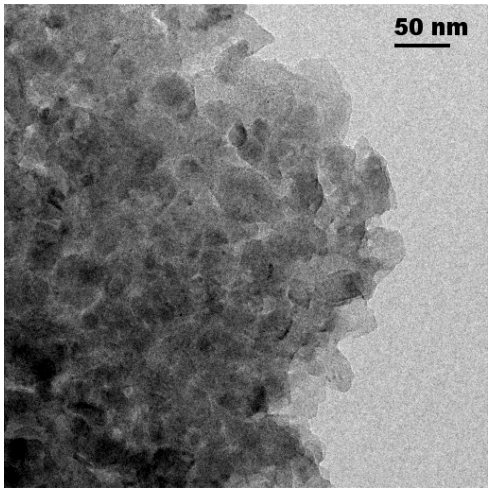

Figure 3.5. TEM Images of (a) FSP3-CaO, (b) HTC $CaCO_3$-CaO, (c) FSP3-CaO after one cycle at 973 K, and (d) HTC $CaCO_3$-CaO after one cycle at 973 K. Images indicate that FSP-CaO sorbents are nanoparticles, and both FSP-, and $CaCO_3$-CaO sorbents sintered after reactions.

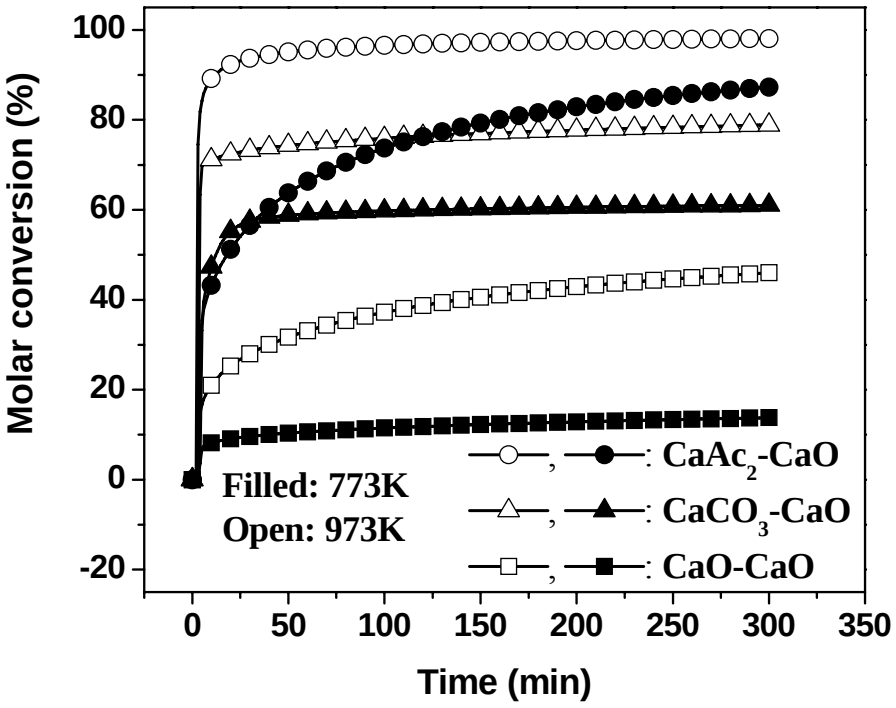

Figure 3.6. Conversion of three HTC-made sorbents at 773 K and 973 K, respectively, indicating the high SSA and porous structure of the $CaAc_2$-CaO sorbents related to their high performance.

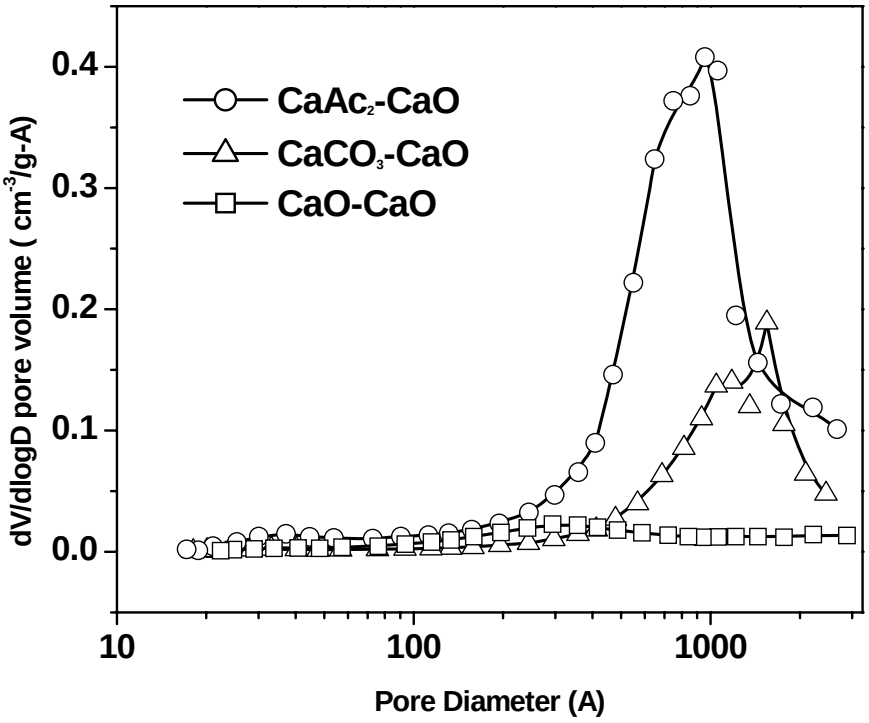

Figure 3.7. Pore size distribution of HTC-made sorbents from various precursors.

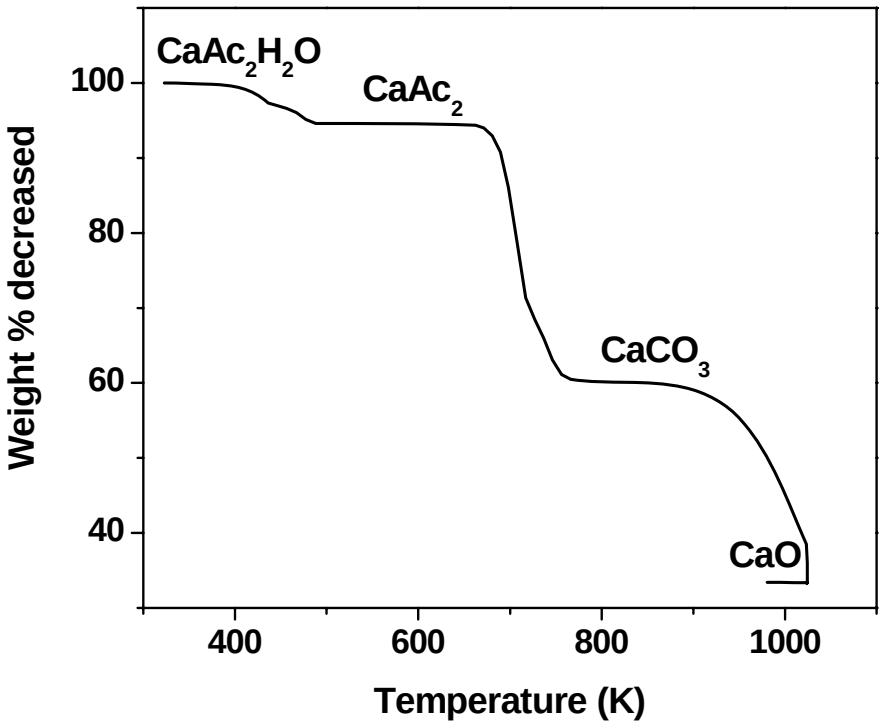

Figure 3.8. Thermogravimetric analysis of $CaAc_2 \cdot H_2O$ sorbent calcination indicating that its characteristic structure arose from specific multi-step decompositions.

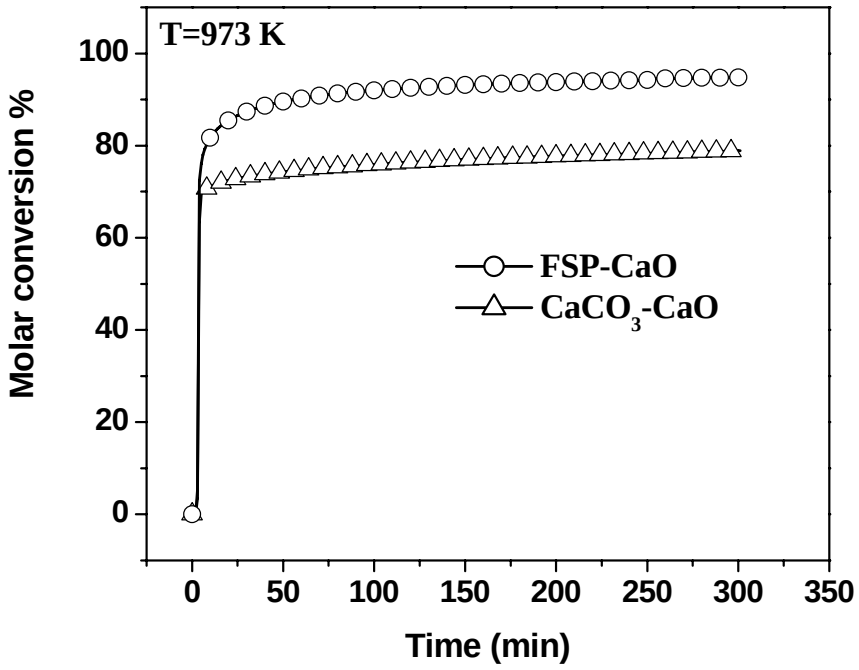

Figure 3.9. Conversion of FSP3-CaO and $CaCO_3$-CaO at 973 K indicating that the high SSA of the former induced the fast reaction and high conversion.

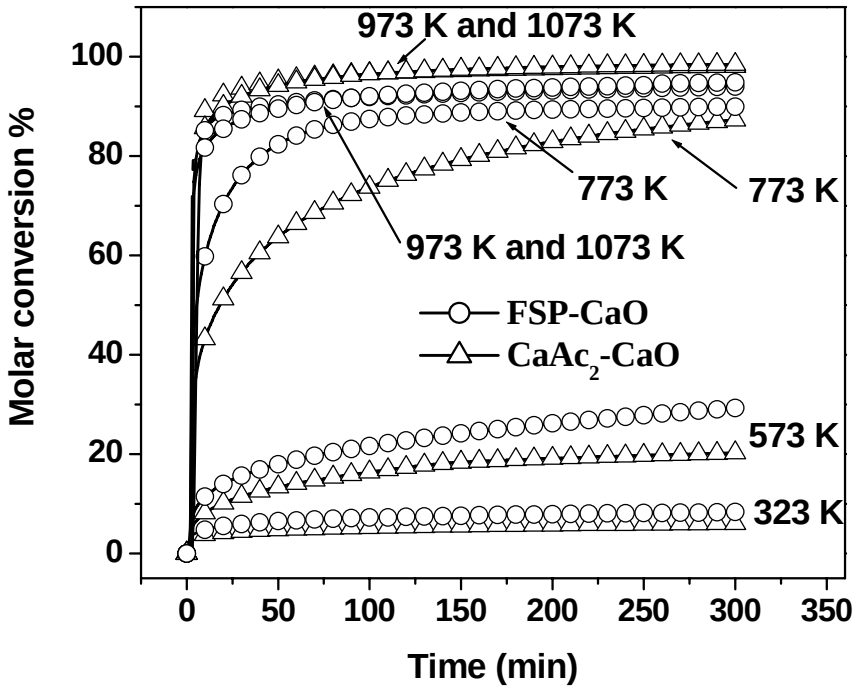

Figure 3.10. Uptake of CO_2 by FSP3-CaO and $CaAc_2$-CaO at various temperatures.

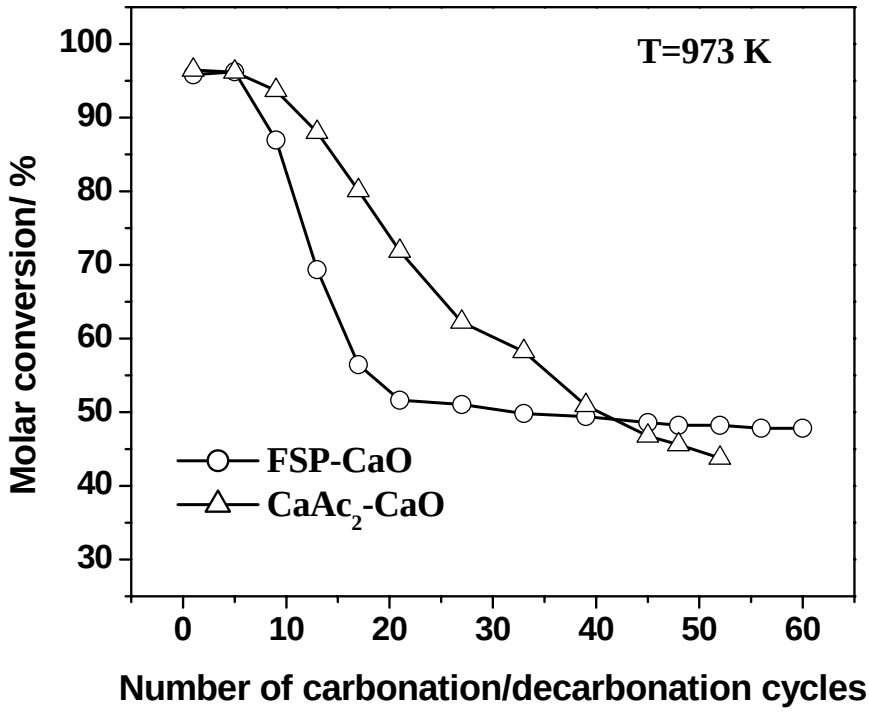

Figure 3.11. Carbonation/decarbonation (300 min/30 min) cycles on FSP3-CaO and $CaAc_2$-CaO at 973 K showing that the former sustained carbonation around 50% after the 20^{th} cycle

Chapter 4. Study on Enhancing the Structure Stability of the CaO Sorbents

Executive summary

To promote reversibility of FSP-made calcium sorbents, silica, titania, and zirconia were selected as dopant. Sorbents with various ratios of these dopants to calcium were synthesized by FSP. The sorbents doping with zirconia (Zr/Ca=3:10 by molar) gave best performance among all sorbents. Except sorbents having Zr/Ca=3:10, all other Si/Ca, Ti/Ca, and most Zr/Ca sorbents showed performance deterioration during long term running. The one having Zr/Ca =3:10 demonstrated stable performance which showed calcium conversion stable around 64% during 102-cycle operations at 973 K.

4.1. Experimental.

Flame spray pyrolysis. CaO sorbent was synthesized with flame pyrolysis method. Calcium oxide precursor and structure promoter precursors mixing in xylene were fed into reactor through syringe pump at a rate of 2 ml/min. The precursors were dispersed by oxygen gas (5 L/min) before it combusted with premixed oxygen/methane. Sorbents were collected at filter locating above reactor.

Chemisorption characterization. Please refer to chapter 3.2.4. CO_2 chemisorption characterization.

4.2. Results and Discussion

The sorbents have BET surface areas about 70 m^2/g and pore volumes more than 0.2 cm^{-3}/g (Table 4.1). Unlike sorbents synthesized by calcining calcium precursors at high temperature, which resulted in porous sorbent, this sorbent is in solid particle form. We propose that the big surface area of this sorbent is ascribed to its large surface areas and pore volumes.

Flame-made sorbents demonstrated good CO_2 capacity and durability in the cyclic operation in chapter 3 of this report. To examine durability of the flame-made sorbents with zirconia, silica, or titania as structure promoter, long term running of sorbents with the same ratio of promoter to calcium (1:10 by molar) were performed. One can observe from Figure 4.1 that performance of all sorbents started to decrease after two dozens to three dozens cycles. The Si/Ca started to decrease first, and had the lowest conversion. At first cycles, Ti/Ca and Zr/Ca had similar high conversion of about 85%, but Si/Ca began to decrease much earlier than Zr/Ca and had apparently lower conversion after 102 cycles of operation. The performance decrease is probably caused by decrease of void space among solid particles.

Since Zr/Ca (1:10) exhibited better performance than Ti/Ca (1:10) and Si/Ca (1:10), performance of Zr/Ca sorbents having different ratios of Zr/Ca were examined. One can observe (Figure 4.2) that the higher ratio of Zr/Ca the sorbent has, the earlier its performance started to decrease, and the faster it did. An exciting observation was that there's no apparent performance decreasing during 102 cycles operation when the ratio between zirconia and calcium oxide is 3 to 10 (Figure 4.A1). The Zr/Ca sorbent (3:10) exhibited better durability than others and its uptake capacity was stable around 64% by calcium molar conversion, or around 30% by sorbent weight during the long term running. It seems that the refractory zirconia of this flame sorbents circumvented

the problem of pore structure collapse and blockage, which caused pore sorbents to deteriorate in the cyclic operation.

An interesting observation is that the Zr/Ca sorbent (3:10) also exhibited stable performance at 823 K, giving performance of around 56% by calcium molar conversion, or 27% by sorbent weight, both of which are less than those at 973 K (Figure 4.A2).

4.3. Conclusions

The sorbents doping with zirconia gave best performance among sorbents having different dopants. All Si/Ca, Ti/Ca, and most Zr/Ca sorbents showed performance deterioration during long term running except for the Zr/Ca (3/10). The one having Zr to Ca of 3:10 by molar gave stable performance. The calcium conversion kept stable around 64% during 102-cycle operations at 973 K. When carbonation was performance at 823 K, the Zr/Ca sorbent (3:10) exhibited stable performance of 56% by calcium molar conversion, or 27% by sorbent weight, both of which are less than those at 973 K as expected.

Table 4.1. BET surface areas and pore volumes of Zirconia promoted flame made sorbents

Zr : Ca (by Atomic)	BET [m^2 g^{-1}]	Pore Volume [cm^3 g^{-1}]
1:10	74	0.23
2:10	67	0.23
3:10	70	0.29

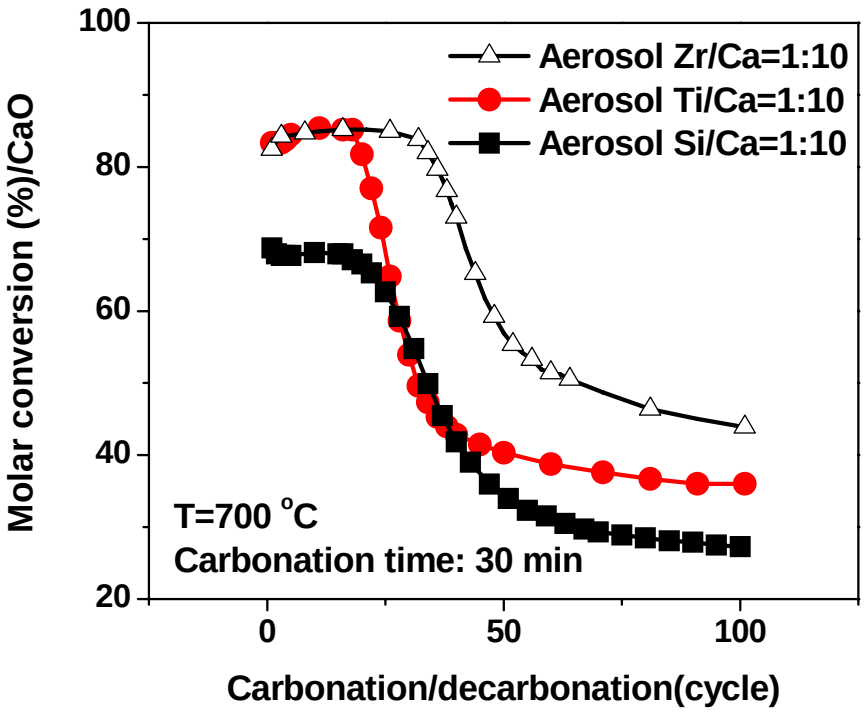

Figure 4.1. Carbonation/decarbonation (30 min/30 min) cycles on Si/Ca(1/10), Ti/Ca(1/10), and Zr/Ca(1/10) sorbents at 973 K showing that the Zr doped sorbents have better performance both in conversion and durability.

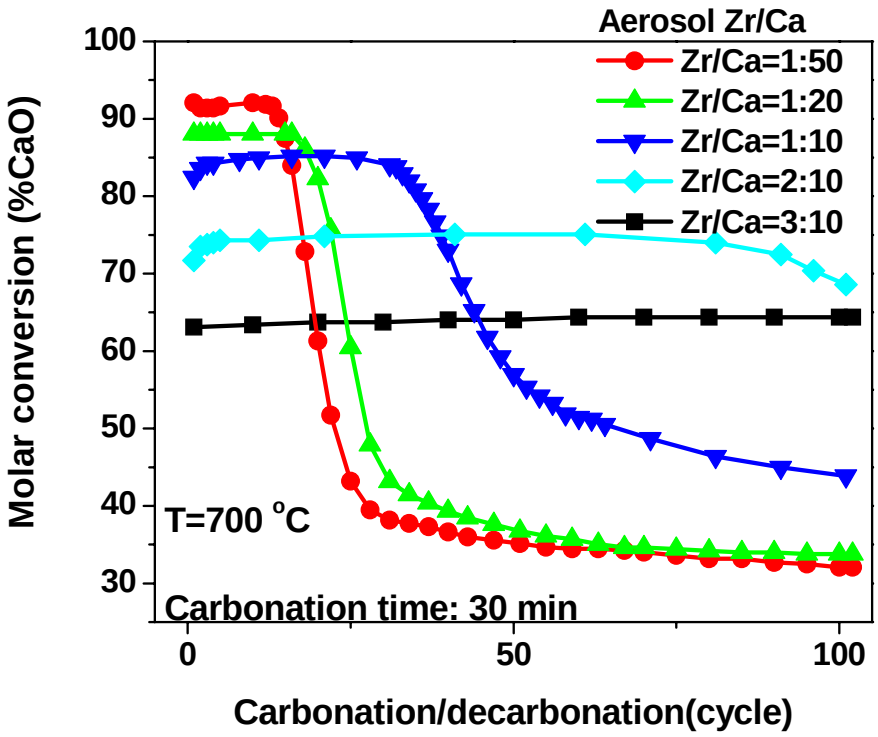

Figure 4.2. Carbonation/decarbonation (30 min/30 min) cycles on flame-made Zr/Ca sorbents having various Zr/Ca ratios at 973 K showing that a sorbent's performance could be stable even after 102-cycle running when it has a Zr/Ca ratio of 3/10.

Appendices

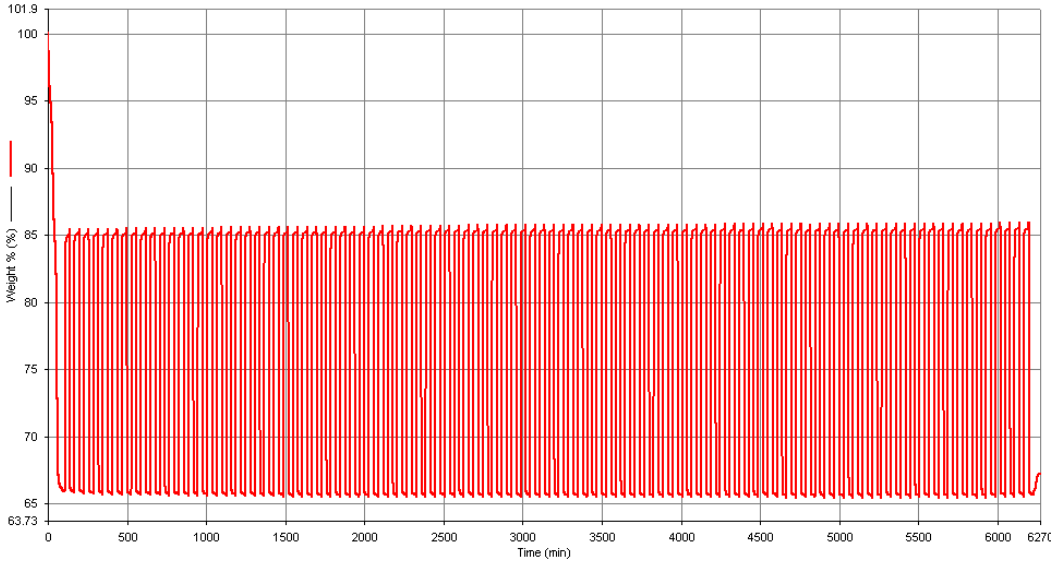

Figure 4. A1. 102 Operation cycles with ZrO_2/CaO made by flame(original TGA figure).
Sorbent: Zr/Ca=3:10 (atomic ratio);
Carbonation /decarbonation temperatures: 973 K (700 ^{o}C);
Carbonation/decarbonation time: 30 min/30 min.

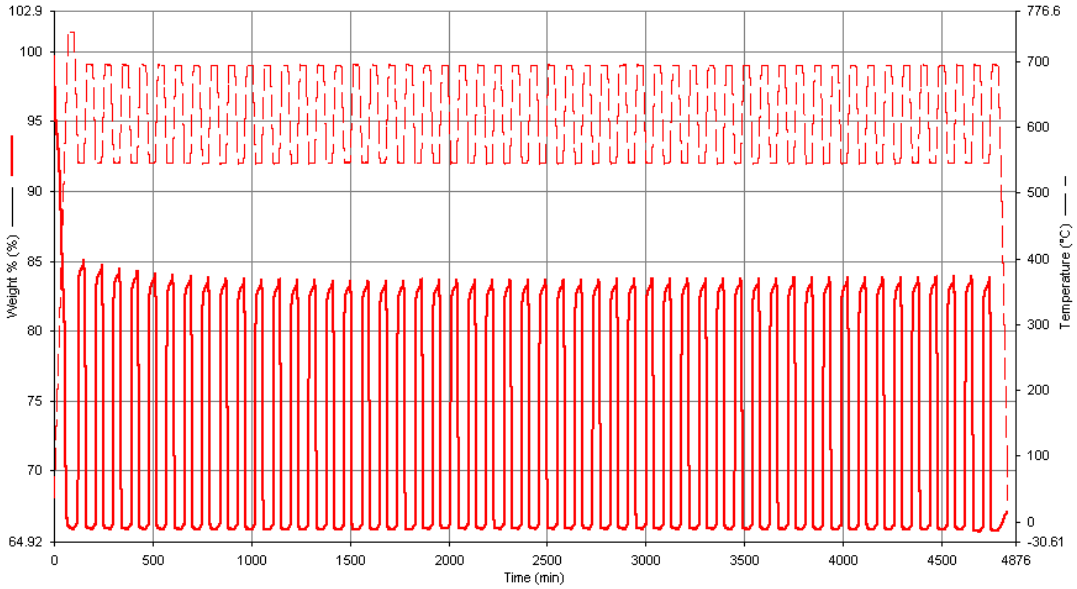

Figure A2. 52 Operation cycles with Zr/Ca made by flame: original TGA figure.
Sorbent: Zr/Ca=3:10 (atomic ratio);
Carbonation /decarbonation temperatures: 550 ^{o}C/700 ^{o}C (823 K/973 K);
Carbonation/decarbonation time: 30 min/30 min.
Solid line: sorbent percent weight;
Dashed line: temperature.

Chapter 5. Study of CaO Sorbents Capturing CO_2 at Severe Conditions [1: higher temperatures and shorter duration period, and 2: with existence of SO_2]

Executive Summary

Calcium-based carbon dioxide sorbents were developed in the gas phase by flame spray pyrolysis (FSP) and tested in multiple carbonation/decarbonation cycles, FSP-made sorbents demonstrated stable, reversible and high CO_2 uptake capacity sustaining maximum molar conversion at about 50% even after 40 such cycles indicating their potential for CO_2 uptake.

In order to provide stability of our CaO sorbents in atmospheres containing SO_2, sorbents doped with various metal oxides were synthesized through coprecipitation technique. We observed that the sorbents doped cerium oxide (Ce/Ca=1:10 by molar) gave the best performance among all sorbents. This sorbent exhibited high capacity in capturing CO_2 while they were capable to be regenerated back to original oxides after carbonation. Other sorbents such as Cr/Ca, Co/Ca, Cu/Ca, and Mn/Ca showed worse performance to capture CO_2 and also failed to achieve complete regeneration back to oxides after carbonation.

The performed work constitutes about 100% of the proposed work and offers a screening for effectiveness in conjunction with the most important operating parameters under realistic conditions.

5.1. Experimental

5.1.1. Sorbent synthesis by FS. Please refer to *3.2.1. Sorbent synthesis by FSP*.

5.1.2 Sorbent synthesis by coprecipitation technique

Ammonium molybdate (Aldrich), and ceric ammonium nitrate (Fisher) were used as dopant precursors. Calcium nitrate tetra hydrate (Fisher) was used as calcium oxides precursor. A serial of other metal precursors were also used as dopant source, . of which all are metal nitrate from Fisher except otherwise described. Calculated amount of precursors were dissolved in 200 ml DI water first, and then 200 ml ammonia carbonate solution containing suitable amount of ammonia carbonate were drop wisely added into above solution to produce precipitants. Liquid mixer was kept stirred rigorously during the whole reaction. The slurry was aged one day before filtration. Solid mixture was calcined one hour at 1173 K under air atmosphere with temperature ramp of 10 C/min during heating up from RT to 1173 K or cool down;

5.1.3. Materials characterization

X-ray diffraction (XRD) measurements were employed for the identification of phases of the synthesized CaO sorbents. The XRD analyses were conducted on a Siemens D500 powder X-ray diffractometer with a Cu KR radiation source (wavelength) 1.5406 Å). An aluminum holder was usedto support the samples in the XRD measurements.

5.1.4. CO_2 chemisorption characterization

All carbonation/decarbonation experiments were conducted by a Perkin-Elmer Pyris™-1 thermogravimertic analyzer (TGA). This TGA was assisted by a Perkin Elmer thermal analysis gas station (TFGS) and Pyris™ v3.8 software. The TGA microbalance resolution is 0.1 μg. To maintain the TGA balance accurately, 45 mL min^{-1} of helium (prepurified, Wright Bros, Inc.) flowed over both balance and sample. The four gas channels of the TFGS can be controlled automatically to introduce reaction gas or balance inert gas into the system.

The carbonation and decarbonation experiments, including heating, cooling, and switching gases between CO_2 (99.5%, Wright Bros, Inc.) and helium were programmed and operated batchwise. Sorbents (ranging from 2 to 10 mg) were placed in a platinum sample holder and heated to the desired carbonation temperature at 10 K min^{-1} under 65 mL min^{-1} flow of helium (45 mL min^{-1} purge gas and 20 mL min^{-1} balance gas). Once the sample reached the carbonation temperature, 20 mL min^{-1} helium was replaced by 20 mL min^{-1} CO_2 initiating the carbonation. The carbonation time was 60 while the decarbonation time 30 min. When SO_2 was feed, 4% SO_2 (in helium) was used as sulfur oxide gas source. Sorbent weight and temperature were recorded continuously throughout the experiment. Rather long reaction times were selected to test the stability of these sorbents which is a crucial characteristic for their large scale application.

5.2. Results and discussion

Sorbents made by flame spray pyrolysis (Table 3.1) shows high capacity of more than 50 % after 20 cycles even when the cycling time is reduced to 5-minute-

carbonation / 5-minute-decarbonation at 973 K (a), 1073 K (b) and under dynamic conditions (c: 5 min carbonation at 973 K and ramped decarbonation at 10 K/min from 973 K – 1173 K – 973 K) for the first 20 cycles of FSP1 sorbent (Figure 5.1). This capacity is substantially higher than the 20% after just 20 carbonation/decarbonation cycles reported in the literature. The shorter carbonation/decarbonation periods lead to slightly lower initial values of the molar conversion, however, similar overall values are observed. This is probably due to the fast reaction rate at the initial stage. The sorbents reached conversions of up to 70% within three minutes (Figure 5.2). Extending carbonation time after fast reaction period does not enhance (if not hurt) the overall sorbent performance in longer operation. Increasing decarbonation temperature slightly decreases the molar conversion which may be attributed to sintering effects as discussed above. This demonstrates again that decarbonation at low temperatures (e.g. 973 K) is advantageous in view of industrial application where the sorbent has to withstand many more cycles. Longer carbonation periods did not show higher, if not lower, conversions in the long run. This may be explained by lower chances for sintering at shorter exposure.

A series of metal precursors were used as dopant source. When the sorbents were exposed to a SO_2 free steam during carbonation, the sorbent with cerium oxide dopant exhibited the fastest kinetics for capturing CO_2 (Figure 5.3). The Co/Ca and Cu/Ca sorbents showed the slowest kinetics during carbonation. During the initial stage of carbonation (10 minutes), the weight of the Ce/Ca sorbent increased 40.0%, while that of Mn/Ca increased by 28.0%, for the Cr/Ca, Cu/Ca and Co/Ca sorbents the weight increases were 13.6%, 24.6%, and 11.0%, respectively. During the decarbonation step following the carbonation (60 minutes), all sorbents were regenerated almost completely in helium stream (Figure 5.3).

Figure 5.4 presents curves for the carbonation of sorbents in the presence of SO_2 followed by decarbonation. The carbonation was performed in the presence of 1000 ppmv SO_2 in a 30% vol CO_2 stream (balanced in helium) for 60 minutes. Regeneration was performed in helium atmosphere after carbonation. Each sorbent showed similar kinetics in the carbonation steps (Figure 5.3 and Figure 5.4, respectively). It is remarkable to note that the Ce/Ca sorbent still exhibited the fastest kinetics. However, a distinguishable difference between the carbonations without or with SO_2 (Figure 5.3 and 5.4, respectively) is that all sobents were not completely regenerated during the decarbonation for the case where SO_2 was cofed. The Ce/Ca sorbent showed the least permanent weight increase of only 5.0% (Figure 5.4). This sorbent also exhibited the highest weight change between the carbonation and decarbonation steps. We proposed that the cerium oxide dopant does repel the SO_2 away from reacting with the CaO surface. However, the exact mechanisms behind the results that we observed involving SO_2 are still unknown and need further investigations. The sorbent with manganese oxide demonstrated the highest weight increase during carbonation. However, there is a permanent weight increase of 24.6% of this sorbent after decarbonation. The permanent weight increase indicates the possible formation of large amounts of sulfate species between the sorbent and SO_2.

5.3. Conclusions

CaO sorbents doped with cerium oxides may survive under SO_2 atmospheres by repelling SO_2 away from the sorbent's surface. Sorbent with high surface area and porosity are capable to reach high conversion (70 %) within two minutes and maintain high conversion at severe operating conditions.

Figures

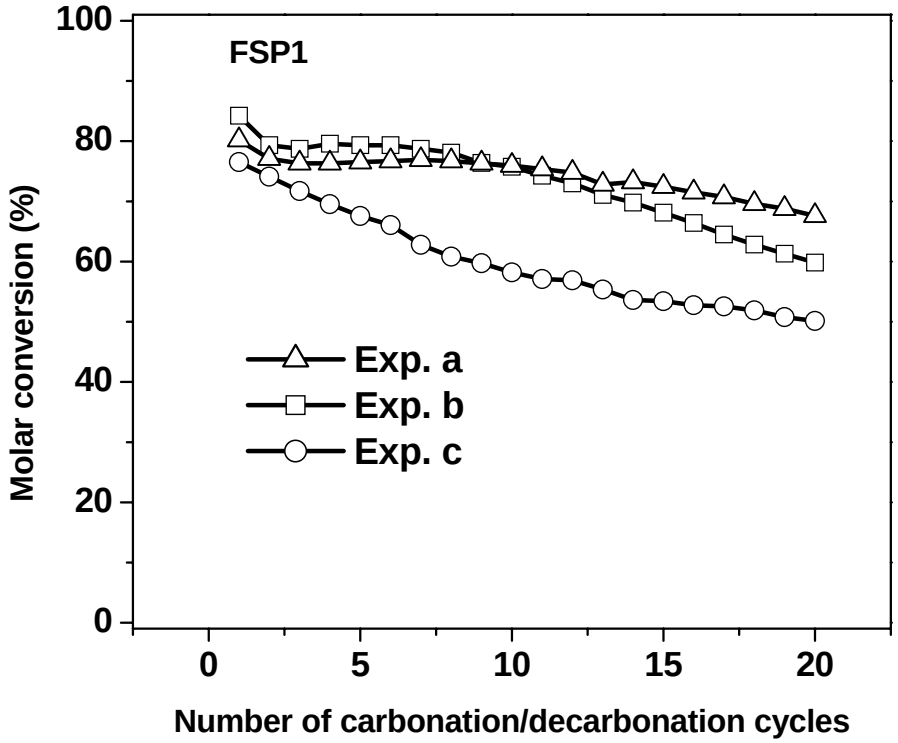

Figure 5.1. Carbonation/decarbonation (5 min/5 min) cycles on FSP1-CaO at a. 973 K, b. 1073 K and c. carbonation for 5 min at 973 and decarbonation for 40 minutes from 973 K to 1173 K and from 1173 K back to 973 K both at 10 K/min. The sorbent could reach high CO_2 capture capacity, be completely regenerated in short time and be quite stable even at higher temperatures.

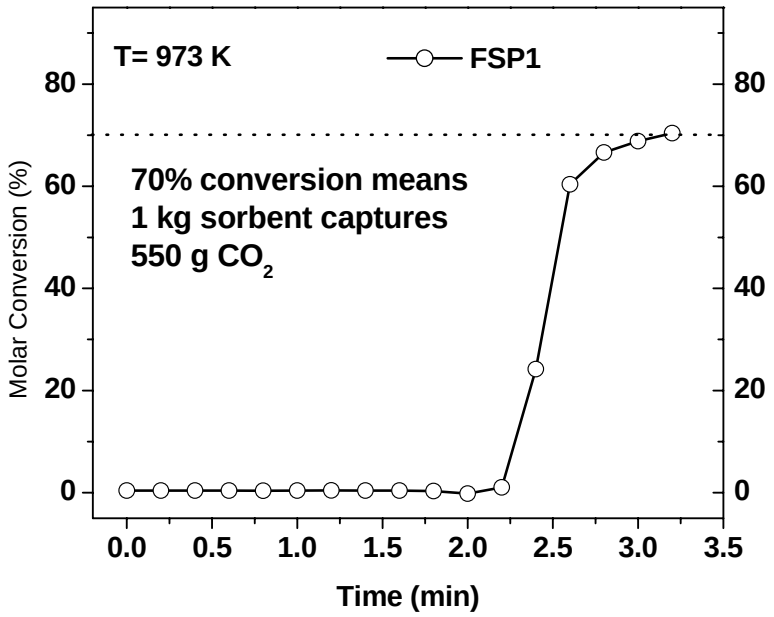

Figure 5.2. Intial carbonation performance of FSP-made CaO sorbent. There was 2 min delay time for CO_2 to reach reactor.

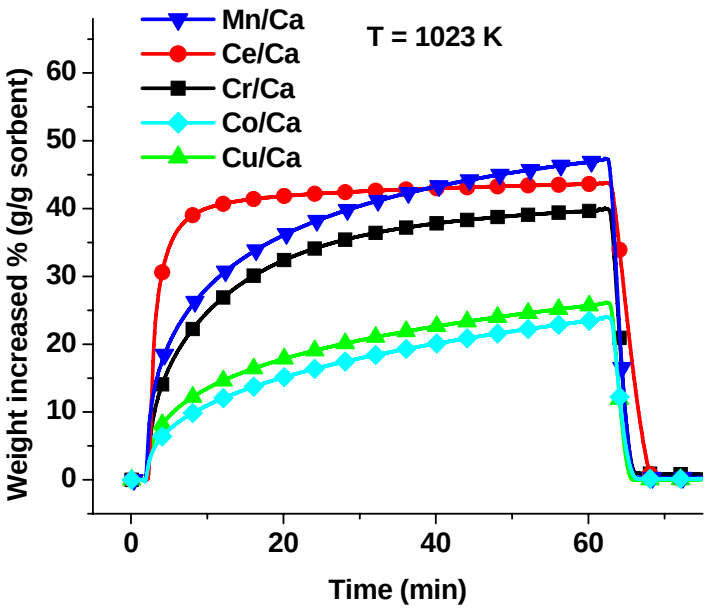

Figure 5.3. M_xO_y/CaO (1/10 by molar) performance at 30 % vol CO_2 Carbonation: 30 % vol CO_2; 1023 K; 60 min. Decarbonation: helium; 1023 K; 30 min.

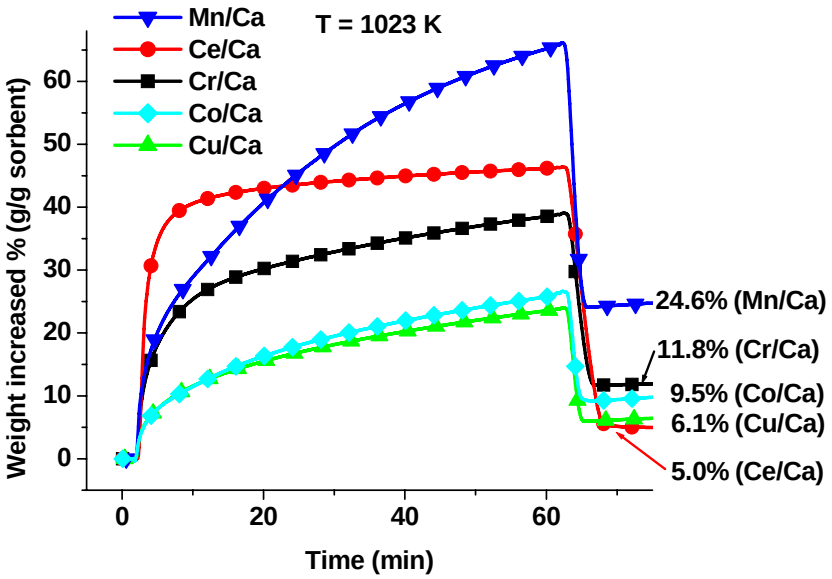

Figure 5.4. M_xO_y/CaO (1/10 by molar) performance at 30 % vol CO_2 and 1000 ppmv SO_2. Carbonation: 30 % vol CO_2, 1000 ppmv SO_2, in helium; 1023 K; 60 min Decarbonation: helium; 1023 K; 30 min.

US Patent Applications, Refereed Articles, Presentations, and Students Receiving Support from this Grant

US Patent Applications
Title: Novel Sorbents for Separaton of CO_2 at a Wide Temperature Range, *Date of submission*; 05/07/2001, *Number*: UC Patent Disclosure 101-020.

Journal Articles (peer reviewed)

1) H. Lu and P. G. Smirniotis; F. O. Ernst and S. E. Pratsinis, "Stable flame-made ca-based sorbents with high carbon dioxide uptake efficiency", submitted to **Chemical Engineering Science**, 2007.

2) H. Lu, A. Khan, and P.G. Smirniotis, "Studies of carbon dioxide sorbents made by organometallic precursors", in preparation for submission to **AIChE Journal** , 2007.

3) H. Lu and P. G. Smirniotis; F. O. Ernst and S. E. Pratsinis, "Zirconia promoted Ca-based sorbents for reversible carbon dioxide uptake at high temperatures", in preparation for submission to **Advanced Materials**, 2007.

4) H. Lu, E. P. Reddy, and P.G. Smirniotis, "Calcium oxide based sorbents for adsorption of carbon dioxide at high temperatures", **Industrial & Engineering Chemistry Research (2006),** vol. 45, p. 3944-3949.

5) A. Roesch, E. P. Reddy, and P.G. Smirniotis, "Parametric Study of Cs/CaO sorbents with respect to simulated flue gases at high temperatures", **Industrial & Engineering Chemistry Research (2005)**, vol 44, p.6485-6490.

Conference Presentations
1) H. Lu and P. G. Smirniotis, "Structure promoted ca-based sorbents for highly reversible carbon dioxide uptake at high temperatures", paper 71d, **AIChE 2006 Annual Meeting** in San Francisco, CA in November, 2006

2) H. Lu, F. O. Ernst, S. E. Pratsinis, and P. G. Smirniotis, "Calcium based CO_2 sorbents made by flame spray pyrolysis and high temperature calcination", paper 439d, **AIChE 2005 Annual Meeting** in Cincinnati, OH in November, 2005

3) H. Lu, .E P. Reddy, and P. G. Smirniotis, "Calcium oxide based sorbents for adsorption of CO_2 at high temperatures", paper 420a, **AIChE 2005 Annual Meeting** in Cincinnati, OH in November, 2005

4-6) This work was also presented at the 2004, 2005 and 2006 Annual Contractors Meeting in Pittsburgh, PA in June 2004, June 2005, and June 2006, respectively.

Students received support from the grant.
Graduate Students:
1) Mr. Hong LU, graduate (Ph.D.) student in Chemical Engineering